AIRUSE-LIFE+: A harmonized PM speciation and source apportionment in 5 Southern European cities

F. Amato[1], A. Alastuey[1], A. Karanasiou[1], F. Lucarelli[2], S. Nava[2], G. Calzolai[2], M. Severi[3], S. Becagli[3], V.L. Gianelle[4], C. Colombi[4], C. Alves[5], D. Custódio[5], T. Nunes[5], M. Cerqueira[5], C. Pio[5], K. Eleftheriadis[6], E. Diapouli[6], C. Reche[1], M.C. Minguillón[1], M. Manousakas[6], T. Maggos[6], S. Vratolis[6], R.M. Harrison[7,8] and X. Querol[1]

[1]Institute of Environmental Assessment and Water Research (IDAEA-CSIC), Barcelona, 08034, Spain
[2]Dep. of Physics and Astronomy, Università di Firenze and INFN-Firenze, Sesto Fiorentino, 50019, Italy
[3]Dep. of Chemistry, Università di Firenze, Sesto Fiorentino, 50019, Italy
[4]Environmental Monitoring Sector, Arpa Lombardia, Via Rosellini 17, I-20124 Milano, Italy
[5]Centre for Environmental & Marine Studies, Dep. of Environment, Univ. of Aveiro, 3810-193 Aveiro, Portugal
[6]Institute of Nuclear and Radiological Science & Technology, Energy & Safety, N.C.S.R. Demokritos, 15341 Ag. Paraskevi, Attiki, Greece
[7]School of Geography, Earth & Environmental Sci., University of Birmingham. Edgbaston, Birmingham B15 2TT, UK
[8]Also at: Department of Environmental Sciences / Center of Excellence in Environmental Studies, King Abdulaziz University, PO Box 80203, Jeddah, 21589, Saudi Arabia

Keywords: Southern Europe, PM, urban, source apportionment

Correspondence to: fulvio.amato@idaea.csic.es

Abstract

The AIRUSE-LIFE+ project aims at characterising similarities and heterogeneities in PM sources and contributions in urban areas from the Southern Europe. Once the main PMx sources are identified, AIRUSE aims at developing and testing the efficiency of specific and non-specific measures to improve urban air quality. This article reports the results of the source apportionment of PM10 and PM2.5 conducted at three urban background sites (Barcelona, Florence and Milan, BCN-UB, FI-UB, MLN-UB) one sub-urban background site (Athens, ATH-SUB) and one traffic site (Porto, POR-TR). After collecting 1047 PM10 and 1116 PM2.5 24h samples during 12 months (from January 2013 on) simultaneously at the 5 cities, these were analysed for the contents of OC, EC, anions, cations, major and trace elements and levoglucosan. The USEPA PMF5 receptor model was applied to these datasets in a harmonised way for each city.

The sum of vehicle exhaust (VEX) and non-exhaust (NEX) contributes within 3.9-10.8 μg/m^3 (16-32%) to PM10 and 2.3-9.4 μg/m^3 (15-36%) to PM2.5, although a fraction of secondary nitrate is also traffic-related but could not be estimated. Important contributions arise from secondary particles (nitrate, sulphate and organics) in PM2.5 (37-82%) but also in PM10 (40-71%) mostly at background sites, revealing the importance of abating gaseous precursors in designing air quality plans.

Biomass burning (BB) contributions vary widely, from 14-24% of PM10 in POR-TR, MLN-UB and FI-UB, 7% in ATH-SUB to <2% in BCN-UB. In PM2.5, BB is the second most important source in MLN-UB (21%) and in POR-TR (18%), the third one in FI-UB (21%) and ATH-SUB (11%), but again negligible (<2%) in BCN-UB. This large variability among cities is mostly due to

the degree of penetration of biomass for residential heating. In Barcelona natural gas is very well supplied across the city and used as fuel in 96% of homes, while, in other cities, PM levels increase on an annual basis by 1-9 $\mu g/m^3$ due to biomass burning influence. Other significant sources are:
- Local dust, 7-12% of PM10 at SUB and UB sites and 19% at the TR site, revealing a contribution from road dust resuspension. In PM2.5 percentages decrease to 2-7% at SUB-UB sites and 15% at the TR site.
- Industry, mainly metallurgy, contributing 4-11% of PM10 (5-12% in PM2.5), but only at BCN-UB, POR-TR and MLN-UB. No clear impact of industrial emissions was found in FI-UB and ATH-SUB.
- Natural contributions from sea salt (13% of PM10 in POR-TR but only 2-7% in the other cities) and Saharan dust (14% in ATH-SUB), but less than 4% in the other cities.

During high pollution days, the largest source (i.e. excluding secondary aerosols factors) of PM10 and PM2.5 are: VEX+NEX in BCN-UB (27-22%) and POR-TR (31-33%), BB in FI-UB (30-33%) and MLN-UB (35-26%) and Saharan dust in ATH-SUB (52-45%) During those days, there are also quite important industrial contributions in BCN-UB (17-18%) and local dust in POR-TR (28-20%).

1.Introduction

Atmospheric particulate matter (PM) concentrations can vary widely across Europe due to different climatic conditions and local features such as anthropogenic source types, emission rates and dispersion patterns. Urban PM10 concentrations show significant variability across Europe as reported by routine monitoring networks (EEA, 2013) and research studies (Querol et al., 2004; Putaud et al., 2010; Lianou et al., 2011; Kukkonen et al., 2005; Karanasiou et al., 2014). For PM2.5 the spatial variability across Southern Europe is less known because in most air quality zones it is not as widely measured as PM10. As a consequence, there is limited information on the geographical variability of the coarse fraction (PM10-2.5), which is often linked to local sources and whose evidence of health concern is increasing (Brunekreef and Forsberg, 2005).
Comparability of data is also hampered by the fact that most research studies analyzed PM data from different periods or with different sampling calendars. An example of this is given by the multi-city studies aimed at investigating the short and long-term health effects of exposure to PMx mass concentrations, NO_x and SO_2 (Eeftens et al., 2012; Medina et al., 2004; Meng et al., 2013; Romieu et al. 2012).
Moreover, the comparison of bulk PM concentrations only, without the necessary chemical characterisation of collected samples and source apportionment analysis, does not allow for an in depth investigation of sources limiting the scope for air quality management purposes.
Recent studies have reported the PM10 and PM2.5 concentrations across Europe but no information on PM composition and sources was provided (Karanasiou et al., 2014; Lianou et al., 2011). In another study, Querol et al. (2004) compared the PM10 and PM2.5 levels and chemistry of seven selected EU regions but datasets were not simultaneous, from 1998 to 2002. The ESCAPE project (Eeftens et al., 2012) investigated the health effects of long-term exposure to ambient air pollution across Europe. PM2.5, PM10 and particle composition were compared at 20 sites across 2008-2011, but measurements were done 3 times for 14 days in different seasons without covering the full year period.
The AIRUSE LIFE+ project generated the first harmonised dataset of Southern European cities for PM10 and PM2.5 levels and composition, following the same sampling protocol and 12 months calendar in Barcelona (Spain), Porto (Portugal), Florence and Milan (Italy), and Athens (Greece). The goal is to characterise the similarities and heterogeneities in PM sources and contributions across the Mediterranean region. This article describes the source apportionment results for PM10

and PM2.5, highlighting common features and dissimilarities across Southern Europe. Once the main sources of PM10 and PM2.5 are identified, the strategic goal of the AIRUSE project is to test and develop specific measures to improve air quality in Southern Europe, targeted to meet air quality standards and to approach as closely as possible the WHO guidelines.

2.Methods

2.1. PM sampling

PM sampling was carried out from January 2013 during 12 months, simultaneously at five sites in Barcelona, Porto, Florence, Milan and Athens. PM10 and PM2.5 24h samples were collected simultaneously every third day. Furthermore, in order to evaluate the chemical fingerprint of Saharan dust, additional PM10 and PM2.5 sampling was performed at each city under selected Saharan dust intrusions after forecasting the occurrence of this phenomenon. The forecast was based on the interpretation of: i) air mass back trajectories calculated with the HYSPLIT4 model from NOAA (Draxler and Rolph, 2003); ii) predictions of dust concentrations by the SKIRON model, University of Athens (http://forecast.uoa.gr.html) and Barcelona Supercomputing Center (NMMB/BSC-Dust forecasts) prediction models.

The details of each monitoring site and instrumentation used are described below:

- BCN-UB: Barcelona urban background (Spain). This is an urban background (UB) site located within the University Campus (South West part of the city) and part of the local air quality network. The nearest trafficked road (Diagonal Avenue, 90,000 vehicles/day) is located 200 m away. PM10 and PM2.5 were collected by means of sequential DIGITEL DH1080 high volume samplers (30 m^3/h) on 150 mm diameter quartz fiber filters at the Palau Reial station (41º23´14´´N, 2º6´56´´E).
- POR-TR: Porto traffic (Portugal). The urban traffic (TR) station is located in Praça Francisco Sá Carneiro (41º09´46.10´´ N; 8º35´26.95´´ W) and part of the National Air Quality Network, QualAr. It is located in the eastern side of Porto city, next to the Fernão de Magalhães Avenue and at 600 meters from the Inner Circular Motorway. Two low volume samplers (TECORA) operating at 2.3 m^3/h collected PM10 and PM2.5 onto 47 mm diameter Teflon filters. A high volume sampler operating at a flow of 1113 l/min with impaction plates from Sierra-Anderson, which enabled the simultaneous collection of PM2.5 and PM2.5-10 onto quartz fibre filters, was used in parallel.
- FI-UB: Florence urban background (Italy). The urban site Bassi is an air quality UB monitoring station (43°47'8.33"N, 11°17'13.19"E) of the Environmental Protection Agency of Tuscany. PM10 and PM2.5 samples were collected by means of two low volume (2.3 m^3/h) CEN equivalent sequential samplers (HYDRA Dual Sampler); each sampler is equipped with two inlets so that aerosol can be simultaneously collected on Teflon membrane and quartz microfibre filters (47 mm diameter, Pall R2PJ047 and Aquaria QF1, respectively).
- ATH-SUB: Athens sub urban background (Greece). This station is part of the Global Atmosphere Watch network (GAW-DEM) and is located in NCSR “Demokritos” campus (37°.99’50’’N 23°.81’60’’E), at the North East corner of the Greater Athens Metropolitan Area and at an altitude of 270 m a.s.l. The suburban site is away from direct emission sources in a vegetated area (pine). PM10 and PM2.5 samples were collected on Teflon filters by means of low volume (2.3 m^3/h) samplers (Sequential 47/50-CD with Peltier cooler,

Sven Leckel GmbH, Tecora Echo PM sampler and Demokritos EN12341 sampler). PM10 and PM2.5 samples were also collected on quartz microfiber filters by means of high volume samplers (Sequential High-Volume Sampler CAV-A/MSb, MCV, SA).

- MLN-UB: Milan urban background (Italy). The Milano Pascal urban background station is part of the ARPA Lombardia Air Quality Network, and it is one of the Italian Supersites for the Italian Decree 155/2010 (Italian transposition of 2008/50/CE). It is located in the eastern side of Milan, the University area called "Città Studi" (45º28´44´´ N, 9º14´07´´ E), in a playground about 130 m from the road traffic. PM10 and PM2.5 were collected on Teflon (Pall), Mixed Cellulose Ester (MCE, Advantec) and quartz microfiber (Pall) filters (47 mm diameter), with five low volume US-EPA reference method samplers (TECORA).

2.2. Sample treatment and analysis

Before sampling, quartz or PTFE microfibre filters were dried for 5 h and conditioned for 48 h at 20 ºC and 50% of relative humidity. Weights of blank filters were measured three times every 24 h by means of a microbalance (1 or 10 µg sensitivity). After weighing, Ø47mm filters were kept in Petri holders, while Ø15cm and large rectangular filters were kept in aluminum foils. After sampling, filters were brought back to the laboratory to be weighed two more times every 24 hours of conditioning at the same temperature and relative humidity as the first weighing.

Once the weights of samples were determined, filters were destined for several analytical determinations. These procedures are briefly listed below, according to the different species analysed:

- Major and trace elements were determined:
    - In Teflon filters by different techniques: PIXE (Particle Induced X-Ray Emission), without any pretreatment (Lucarelli et al., 2014); after acid digestion (5 ml HF, 2.5 ml HNO_3, 2.5 ml $HClO_4$) of 1/2 of each filter, consecutively by ICP-MS (Inductively Coupled Plasma Mass Spectrometry) and ICP-AES (Inductively Coupled Plasma Atomic Emission Spectroscopy) (Querol et al., 2001) to assure comparability between the two techniques (only for Porto samples, Figure S1); by ICP-AES after digestion with HNO_3-H_2O_2 in a microwave oven according to the EU method EN14902:2005 (Traversi et al., 2014), only for Florence samples (Figure S1); by XRF (X-Ray Fluorescence) with polarized primary X-Ray beam and several secondary targets, after an intercomparison with PIXE (Figure S2), only for Milan samples (Table S1);
    - In quartz filters by ICP-MS and ICP-AES after acid digestion (5 ml HF, 2.5 ml HNO_3, 2.5 ml $HClO_4$) of 1/4 of each filter (Querol et al., 2001) (Table S1);
    - In Teflon and MCE filters by XRF (X-ray Fluorescence), only for Milan samples.

- Water soluble ions by IC (Ion Chromatography), after extraction in 20 ml of MilliQ water (with ultrasonic bath for 30 min) of ½ or ¼ of filter;
- On quartz filters organic carbon (OC) and elemental carbon (EC) by thermal-optical analysis with the EUSAAR2 temperature program by means of Sunset analyzers. Filters from POR-TR were analysed in a thermal-optical transmission system described in detail elsewhere, following a similar protocol of EUSAAR2 (Pio et al., 1998, 2011).

- On the PM10 quartz microfibre filters, Carbonate Carbon (CC), by means of the procedure described by Pio et al. (1994): briefly, the carbonate measurement setup comprises four components: a mass flow meter, a reaction cell, an infrared CO_2 analyser, and a computer terminal for data acquisition. A portion of each filter (9 mm punches) is acidified with orthophosphoric acid (20%) in a CO2 free gas stream to convert the carbonate carbon to CO_2, which is then detected by an infrared analyser.
- On the PM2.5 quartz filters, levoglucosan was determined by means of IC after extraction in 10 ml of MilliQ water (with ultrasonic bath for 30 min) on 1.5 cm² punch of filter (Table S1).

The ICP-MS, PIXE, GC-MS, CC, XRF analysis were carried out by one laboratory for each technique, while IC and ECOC analysis were separated among the five laboratories.

2.3. Source apportionment

Source apportionment studies of atmospheric particulate matter are often performed by means of receptor models that are based on the mass conservation principle:

$$x_{ij} = \sum_{k=1}^{p} g_{ik} f_{jk} + e_{ij} \qquad i=1,2,\ldots,m \quad j=1, 2\ldots. n \qquad (1)$$

where x_{ij} is the concentration of the species j in the i^{th} sample, g_{ik} is the contribution of the k^{th} source in the i^{th} sample, f_{jk} is the concentration of the species j in source k *and* e_{ij} is the error of each individual data. Equation (1) can be also expressed in matrix form as $\mathbf{X}=\mathbf{GF}^T$. If f_{jk} are known for all the sources then the Chemical Mass Balance (CMB) can be applied (Watson et al., 1984), as for this model the experimental profiles of all major sources are needed. When both g_{ik} and f_{jk} are unknown, factor analysis (FA) techniques such as *Principal Components Analysis* (PCA) (Thurston and Spengler, 1967; Henry and Hidy, 1979) and *Positive Matrix Factorisation* (PMF) (Paatero and Tapper, 1994) are used for solving equation (1). PMF can be solved with the Multilinear Engine (ME-2) developed by Paatero (1999) and implemented in the version 5 of the US EPA PMF (http://www.epa.gov/heasd/research/pmf.html).

In this study, the US EPA PMF v5 was applied to the five datasets obtained at BCN-UB, FI-UB, ATH-SUB, MLN-UB and POR-TR. Since PMF is a weighted least-squares method, individual estimates of the uncertainty in each data value are needed. The uncertainty estimates were based on the approaches by Polissar et al. (2008), Amato et al. (2009) and Escrig Vidal et al. (2009). Species which retain a significant signal were separated from the ones dominated by noise, following the signal-to-noise (S/N) criterion defined by Paatero and Hopke (2003). Species with S/N<0.2 are generally defined as bad variables and removed from the analysis and species with 0.2< S/N < 2 are generally defined as weak variables and down weighted (increasing uncertainty by a factor of 3. Nevertheless, since S/N is very sensitive to sporadic values much higher than the level of noise, the percentage of data above detection limit was used as complementary criterion.

In those cases where the PMF model was not able to resolve a Saharan dust source, the Saharan dust contribution was estimated according to the methodology proposed by SEC (2011).

3. Results and Discussion

3.1. PM10 and PM2.5 levels

As shown in Table 1, the observed mean PM levels during the study period were as follows:

- PM10 in the urban background (UB) reached 19-23 μg/m^3 in FI and BCN, and 38 μg/m^3 in MLN. In the suburban background (SUB) site in ATH levels reached 20 μg/m^3, whereas at the traffic (TR) site of POR, concentrations reached 34 μg/m^3.
- For PM2.5, levels reached 13-15 μg/m^3 at the UB sites of FI and BCN, 30 μg/m^3 in MLN, 11 μg/m^3 at the SUB site in Athens, and 27 μg/m^3 in POR-TR.

All sites met EU legal requirements (2008/50/EC) for the annual limit value of PM10 (40 μg/m^3). However, the legal requirement of not exceeding 50 μg/m^3 for the 90.4th percentile of the annual data (daily limit value) was exceeded at MLN-UB (72 μg/m^3) and POR-TR (53 μg/m^3). The annual EU target value of PM2.5 (25 μg/m^3, 2008/50/EC) was exceeded at POR-TR (27 μg/m^3) and MLN-UB (29 μg/m^3). For the UB sites mean PM10 levels are similar with the exception of MLN with relatively higher levels, due to intense local and regional PM source contributions and to the specific meteorology of the Po Valley, with frequent and intensive atmospheric thermal inversions that induce regional accumulation of pollutants.

For PM2.5, similar and relatively lower values (as compared with PM10) were recorded at UB and SUB sites (11-15 μg/m^3), with the exception of MLN (30 μg/m^3). In the case of the TR site, mean level reached 27 μg/m^3. UB and SUB PM2.5/PM10 ratios were close to 0.7 in the case of FI and BCN, 0.5 for ATH and 0.8 for MLN. At POR-TR site it increased to 0.8. Although at the TR site levels of resuspension of road dust (mainly in the coarse size) are expected to be higher than at UB sites, the proximity to the exhaust emissions (dominated by fine PM) results in a higher PM2.5/PM10 ratio.

When considering the stricter WHO guidelines, all cities exceeded both the PM10 and PM2.5 annual mean thresholds, with the exception of PM10 in FI-UB. It is worth noting that the sampling year was particularly rainy in most of the study sites, including Florence. The daily PM10 and PM2.5 WHO threshold (50 and 25 μg/m^3, respectively) was exceeded only in MLN-UB and POR-TR.

As shown by Figure S3, seasonal trends for PM10 at the 5 AIRUSE cities were very different. ATH-SUB was characterised by higher spring-summer and lower autumn-winter PM10 levels probably due to higher African dust influence in the warm seasons. A similar but much smoother trend was observed for BCN-UB. For POR-TR, the highest levels were recorded in summer and the lowest in spring. At MLN-UB, lower levels were recorded in spring and summer, when PM10 levels reached similar levels to BCN-UB, FI-UB or ATH-SUB; however in autumn and winter levels at MLN-UB were higher by a factor of more than 2 with respect to the other seasons and most of the other cities. This is due to the aforementioned atmospheric stagnation features of the Po Valley that favoured the accumulation of intensive winter PM emissions. At FI-UB a similar trend was observed but with a less pronounced winter increase than that described for MLN-UB. In fact, Florence is also located in a closed basin (the Arno river valley), which is characterised by stagnant conditions during the cold season. PM2.5 levels followed similar seasonal patterns to those described above for PM10 at each city.

3.2. PM chemical composition

3.2.1. EC, OC and OM

EC is a tracer of emissions from road traffic, mainly from diesel vehicles (Querol et al., 2013); it is a carrier of highly health relevant organic species (WHO, 2012). Mean EC concentrations reached 1.1 μg/m^3 in PM10 at the UB site of BCN and FI and 1.9 μg/m^3 at the UB site of MLN (Figure 1). At the SUB site of ATH, EC levels were lower (0.4 μg/m^3 in PM10, Figure 1) due to the higher distance from avenues with high traffic load, but also due to the lower proportion of diesel vehicles in the fleet of ATH compared to the other 3 cities. Until 2012, the use of diesel for private cars was not allowed in this city.

As expected, levels of EC at traffic sites were higher than at UB sites by a factor ranging from 3.6 to 4.9. EC levels recorded for PM10 are very close to those of PM2.5 (PM2.5/PM10 ratios within 0.9 to 1.0) pointing to the very fine size of the EC-bearing particles.

OM was calculated by multiplying OC by a factor accounting for non-C atoms which may change according to location and existing sources (Turpin and Huntzicker, 2005). This factor ranged from 1.2 (in POR-TR site due its proximity to traffic emissions, Pio et al., 2011) to 1.7-1.8 (rest of sites, Minguillón et al., 2011 and Mohr et al., 2012). Mean levels of OM (Figure 1) reached 5.0 and 5.5 μg/m^3 in PM10 at BCN-UB and ATH-SUB sites, respectively, but increased up to 9.6 and 15.4 μg/m^3 at FI-UB and MLN-UB. At POR-TR, mean level of OM was 7.9 μg/m^3. OM has also a fine grain size since PM2.5/PM10 ratios for this component ranged from 0.7 to 1.0. OM/EC ratios for PM10 ranged from 1.6 at POR-TR, reaching values of 4.4 at the UB site of BCN, 8.2 and 8.7 at the UB sites of MLN and FI and 13 at the SUB site of ATH. This ratio results from the influence of both the proximity to the emission sources and the biomass burning. Thus, primary diesel soot is characterised by an OM/EC ratio close to 1.0, whereas a higher ratio indicates a major relative abundance of secondary OM, due to a longer distance from emission hotspots (from TR to UB to SUB) and/or a higher contribution from biomass burning to PMx levels, since OM/EC from biomass burning is much higher (Puxbaum et al., 2007). Also biogenic emissions can increase the OM/EC ratio.

Levels of OM+EC accounted for around 27-30% of the PM10 load at the UB and SUB sites, with the exception of FI and MLN (45-58%). At POR-TR this contribution increased to 37%. In PM2.5 the OM+EC load increased as compared with PM10 and reached from 37 to 69% of the PM2.5 mass. This is due mainly to the decrease of mineral dust and sea salt in PM2.5 when compared with PM10.

The higher levels of OM recorded at MLN, FI, and partially at POR, are probably the result of a high contribution to PM10 levels from biomass burning (BB). This is also confirmed by the high OM/EC ratios. In the case of MLN the frequent atmospheric stagnation episodes also favour the formation of secondary OM as also described later for nitrate. To a lesser extent this also applies for FI, where stagnant conditions are common during winter.

3.2.2. Sea salt

Sea salt was calculated based on the main composition of sea spray (ss) as the sum: ssNa + Cl + ssMg + ssK + ssCa + ssSO$_4^{2-}$. where ssNa = Na – nssNa; nssNa = 0.348*Al; ssMg = 0.119*ssNa; ssK = 0.037*ssNa; ssCa = 0.038*ssNa; ssSO4 = 0.253*ssNa (Calzolai et al., 2015). Mean levels of sea salt (Figure 1) in PM10 reached 0.6-0.7 μg/m^3 at the inland Italian cities (FI and MLN, 2-3% of the PM10 load) and 1.5-1.7 μg/m^3 (7-8% of the PM10 load) at the Mediterranean coastal sites.

However, at the Atlantic site (POR) much higher levels were recorded (4.3 μg/m^3 in PM10, 13% of the PM10 load at the TR site).
As expected, due to the coarse mass size distribution of sea salt, levels were reduced by 71-86% in PM2.5 with respect to PM10, with the exception of MLN, where levels of sea salt were only reduced by around 38% in PM2.5.

3.2.3. Mineral dust

Mineral dust (or soil dust) was calculated based on average crust composition (Nava et al., 2012) as: 1.15*(3.79*Al+2.14*Si+1.67*Ti) ¯. In case of quartz filter, a value of 3 for ratio SiO_2/Al_2O_3 was used. Mineral dust at UB sites reached around 2.3 μg/m^3 as annual mean in FI-UB and 3.8-4.2 μg/m^3 at the UB and SUB sites of BCN, MLN and ATH (Figure 1). These levels account for 18% and 25% of the PM10 mass at BCN and ATH and 12 and 10% at FI and MLN, respectively. At POR-TR site mineral dust accounts for 12% of the PM10.
As also expected from the coarse mode of occurrence of mineral dust, levels of this PM component were much lower in PM2.5, down to 20-49% of the PM10 levels. The contribution of mineral dust reached from 4 to 10 % of PM2.5 for all sites.

3.2.4. Sulphate and nitrate

There is a marked geographical variability, with increased levels of sulphate from FI-BCN to POR-MLN to ATH (1.7-2.0 to 2.4-3.0 to 3.7 μg/m^3 in PM10 and 1.5-1.7 to 1.9-2.0 to 2.9 μg/m^3 in PM2.5, Figure 1). This is probably due to the influence of the use of coal and petroleum coke/fuel oil for power generation in or/and around the high sulphate regions of this study, but also it may be caused by the influence of SO_2 emissions from petrochemical plants. In the case of POR, when the site is under the influence of NW winds, one of the major sources of sulphate could be the Porto Refinery (10 km away from the sampling site), which began operating in 1970. It is a crude oil industrial processing plant that has an annual installed capacity of 4.5 million tons and produces a wide range of products including fuels, lubricants, aromatics (BTX) for the petrochemical industry, industrial solvents and petroleum waxes. Emissions from shipping in the harbour may represent another possible source. As expected from the fine mode of occurrence of ammonium sulphate ($(NH_4)_2SO_4$ or NH_4HSO_4), 76% to 85% of sulphate in PM10 is present in PM2.5.
Levels of nitrate in PM10 show a less marked spatial variability, with the exception of MLN, with mean annual levels reaching 1.2 (FI-ATH) to 2.0 (POR-BCN) μg/m^3 and 6.0 μg/m^3 in MLN. This marked difference between MLN and the rest of the other AIRUSE regions is mainly due to the specific meteorological and emission patterns of the Po Valley. In this case, it coincides with a large urban and industrial agglomeration (with the associated road traffic), with the consequent elevated atmospheric emissions and a peculiar meteorology favouring frequent and marked thermal inversions that cause the accumulation of pollutants and the formation of high levels of ammonium nitrate (NH_4NO_3) from the high anthropogenic NO_x and NH_3 emissions and the coldest temperature in winter among AIRUSE cities. In particular, high NH_3 levels, emitted from agricultural and animal husbandry activities, can be transported from the southern part of the Po Valley to the urbanised northern part, inducing ammonium nitrate formation. On the other hand, it is noticeable the relatively coarse mode of nitrate in all cases, since levels in PM2.5 are generally 50-60% lower than in PM10, with the exception of MLN by 40% and the ATH-SUB area by 85%. These large

fractions of coarse nitrate are probably due to the high temperatures and dry conditions reached in summer in the study regions. Especially at higher temperatures, NH_4NO_3 dissociate into gaseous HNO_3 and NH_3, and in turn a fraction of this HNO_3 may react with NaCl or $CaCO_3$ to give coarse $NaNO_3$ or $Ca(NO_3)_2$. This accounts for the large differences observed for nitrate in the coarse and fine size fractions at MLN and ATH, with 60% of nitrate residing in the fine aerosol at the first site and only 15% at the latter. The hypothesis of a temperature-driven behaviour of nitrate is reinforced by the seasonal trends of the ratios between fine (PM2.5) nitrate and PM10 nitrate: most of the nitrate, i.e. 60-80% of it, is in PM2.5 during fall and winter, while the percentage drastically decreases during spring-summer, down to roughly 15%. Seasonal trends are less and less pronounced when passing from cities with a continental climate such as FI (and MLN) to coastal ones with a mild climate such as POR and BCN, and are not visible in ATH, with a warmer climate. The contribution of sulphate, nitrate and ammonium (secondary inorganic aerosols, SIA) to the PM10 load reaches 15-21% of PM10 in BCN-UB, POR-TR and FI-UB, but 30-31% at MLN-UB and ATH-SUB. In spite of the prevailing fine mode of these PM components, the contribution of SIA to the PM2.5 load remains similar to that of PM10, with 13-23% and 31-37% for the above groups of sites. The latter two cities (MLN and ATH) are both characterised by similarly high SIA loads, but due to different causes, whereas at MLN SIA is dominated by ammonium nitrate, in ATH ammonium sulphate prevails.

The ion balances between cations and anions of the daily PM10 and PM2.5 samples collected at the 5 AIRUSE cities are reported in Figure S4. The results showed that there was a neutralisation of the acidic components of the PM10 and PM2.5 in all cases with the exception of FI in the PM2.5 fraction. Thus, the balances range from Anions=0.82*Cations (BCN, R^2=0.72) to Anions=1.0*Cations (POR, R^2=0.96). A slope lower than 1.0 means that there is a cation load in excess, probably due to the occurrence of Ca and Mg-bearing carbonate minerals (Alastuey et al., 2005). This is expected to occur specially during African dust episodes (see low anion/cation samples present in the balance of BCN in Figure S4). In the case of FI PM2.5 samples, the regression fits with Anions=1.12*Cations (R^2=0.95) which points to a slightly acidic character of the PM samples with a fraction of 12% of the anionic species being present as acids. However conclusions on aerosol pH cannot be conclusive given that ionic balance and molar ratio methods have been recently criticized (Hennigan et al., 2015).

3.2.5. Secondary vs primary PM

The amount of secondary aerosol was roughly estimated at each site as:

$$\textit{Secondary aerosols: } NO_3^- + SO_4^{2-} + NH_4^+ + (OC-(EC*a))*b \quad (2)$$

where *a* expresses the primary OC/EC ratio (averaged among existing sources, and varying within 0.7-2.2 (Pio et al., 2011)) and *b* accounts for the non-C atoms in secondary aerosol mass (varying within 1.6-2.1, Aiken et al., 2008). Figure 2 shows that for PM10, at the UB and SUB sites the secondary fraction dominated the PM10 mass by contributing from 53% (BCN) to 71% (MLN), whereas at POR-TR the primary contribution prevailed (60-63%). For the calculation of the secondary and primary fractions all values are normalised by the sum of reconstructed PM mass. This high load of secondary PM mass is very important to be taken into account in designing air quality plans, since these components are formed in the atmosphere from organic and inorganic

gaseous precursors. The organic and inorganic secondary contributions to PM10 are very well balanced (close to 50-50% in most cases), but not in the case of FI-UB, where 65% of the secondary PM10 load is from organic aerosols (Figure 2), indicating probably a relative contribution from biomass burning compared with the other sources. The contributions of secondary aerosols to PM2.5 increase when compared with PM10 due to the lower contributions of dust and sea salt to the fine fraction. This secondary contribution then ranged from 66% (BCN) to 82% (ATH) in the UB and SUB sites and 37% at POR-TR (Figure 2).

3.2.6. Biomass burning tracers

Levels of levoglucosan and K are considered as tracers for biomass burning (Fine et al., 2001, Gonçalves et al., 2010, Nava et al., 2014). In fact, levoglucosan is a sugar emitted into the atmosphere exclusively by breaking cellulose chains during biomass burning. Levoglucosan levels varied by one order of magnitude: 20 (BCN), 37 (ATH), 255 (FI), 274 (MLN) and 387 (POR) ng/m^3 in PM2.5 (Table 1), reflecting a very clear difference of the impact of biomass burning on air quality across southern European cities. The values obtained should be considered as minimum levels because it is well known that levoglucosan may be degraded in highly oxidising environments (Simoneit et al., 1999). This impact is mostly due to differences in using biomass burning for domestic purposes, but also in POR and MLN peak events were detected in summer as a consequence of the impact of the emissions of forest fires and/or agricultural fires. The decreasing impact of biomass burning on PM2.5 levels when passing from MLN to FI to POR to ATH and to BCN is clearly demonstrated by the time series of daily levels of levoglucosan (Table 1). The lower values for Athens can be also attributed to the suburban character of the site. On the other hand, levels of K in the fine fraction (PM2.5) may also increase as a consequence of the influence of inorganic biomass burning ash contributions to the PM load. In this case, the differences are also evident but less marked than for levoglucosan: 87 (BCN), 115 (ATH), 172 (FI), 345 (POR) and 303 (MLN) ng/m^3 in PM2.5 (Table 1). This lower differentiation is due to the fact that K may be partially supplied by mineral dust (clay minerals and feldspars) and probably by specific industrial sources.

3.2.7. Trace elements

Levels of Ti, Mn, Sr, Cu, Zn, Sn, Ni, Ba and Pb are higher in MLN, and in some cases in POR (Zn, Ba, Pb, Cd), when compared with the other sites. Most of these elements are usually related to metallurgy and heavy industry emissions.

Levels of As and Se (generally used as tracers of coal combustion*)* were relatively higher in POR and ATH pointing to a possible local, regional or long range transport influence of emissions from coal combustion sources on air quality. Northern Greece has a number of large coal fired power plants that may partly account for these concentration levels. Transport of emissions from coal fired power plants from the Balkans, Eastern Europe and Turkey may also contribute. In the case of POR, the coal power plant located 15 km southeast of Porto was deactivated in December 2004 and there was no coal combustion activity at the area during the campaign. The closest coal fired power plant is located in Northwestern Spain, at around 300 km from Porto. Is it possible that other industrial sources of As and Se (ceramic, glass, and cement production, among others) may also contribute to increased levels of these elements.

Levels of Cu, Sb, Ba and Sn were relatively higher in POR-TR as compared with UB sites, due to their association with non-exhaust vehicle emissions including brake and tyre wear (Gietl et al., 2010).
Levels of V were 4 to 2 times higher in the cities with a harbour (POR, BCN and ATH) pointing to the fact that, in spite of the possible use of fuel oil or petroleum coke for power generation or industrial processes, shipping emissions are the main sources of these heavy oil combustion tracers in these AIRUSE cities.
Rare Earth Elements (REEs) are usually occurring in mineral dust and the ratio Ce/La in the Earth's crust is close to 2. The marked decrease of this ratio may be used as a tracer of the influence of emission from La-based oil cracking in petrochemical plants. In this study most of the cities have a ratio Ce/La close to 2.0 with the exception of FI and ATH (1.0 and 1.3), this indicating the possible influence of this type of emissions at both sites, although other sources for La cannot be discarded. In Athens the refinery is located 15 km northwest of city center, while in Florence about 90 km away to the West, in the province of Livorno.

The unaccounted mass of PM is that resulting from the difference of the gravimetric measurements of the filters and the sum of all the components determined by chemical analysis. This unaccounted mass is usually attributed to water molecules contained in potential remaining moisture, and crystallisation and formation water (water molecules in the structure of specific chemical species. In this study the unaccounted mass was higher at BCN-UB and POR-TR (23 and 31% for PM10 and PM2.5, respectively) and similarly lower (5-14%) in all the other sites.

3.2.8. Source apportionment results

For each AIRUSE station, the best PMF solution was found when combining PM10 and PM2.5 samples in a single input matrix for PMF. This method is not new, as it was already proven to increase considerably the statistical significance of the analysis, although it assumes that the chemical profiles of sources do not vary between PM2.5 and PM10 (Amato et al., 2009). Depending on site, different constraints were added into the PMF model (Paatero and Hopke, 2008), in order to reduce rotational ambiguity and drive the iterations towards a more realistic solution. Auxiliary equations were therefore introduced, by means of the USEPA software, and included both physical and chemical constraints. Table 2 summarizes the constraints used in each case, as well as the increment of dQ (Amato et al., 2009), i.e. the increase of the object function due to the use of auxiliary equations, which in all cases were accomplished with a total increase in dQ within 3-19%.

The distribution of residuals, G-space plots, Fpeak values and Q values were explored for solutions with number of factors varying between 6 and 11 (USEPA, 2014). Table 2 also lists the factors/source finally identified in each case, which varies within 8 and 10. Factor labelling were kept as generic as possible since perfect decomposition is difficult to achieve and factors represent likely a mixture of different sources and processes (e.g. vehicle non-exhaust). Five factors were commonly found at all sites: Vehicle exhaust (VEX), Vehicle non-exhaust (NEX), Secondary nitrate (SNI), Sea salt (SEA) and Mineral dust (MIN). The Biomass burning (BB) source was also found at all sites, except for BCN-UB where 96% of homes are heated by natural gas. The Secondary sulphate and organics (SSO) factor was separated from the Heavy oil combustion (HOC) only in BCN-UB, FI-UB and ATH-SUB, while in MLN-UB and POR-TR, these two factors were

combined in a composite Heavy oil and secondary (HOS) factor. In addition the IND source was identified at BCN-UB, POR-TR and MLN-UB, while possible industrial contributions in FI-UB and ATH-SUB would be included in the HOC factor. Finally, in FI-UB two sea salt factors (Aged, with influence of the refinery located to the coast and Fresh) and two mineral dust factors (Local and Saharan dust) were separated.

Traffic sources

The NEX source generally shows a mixed composition (Figure 3), including crustal species (Fe, Ca, Al, Si among others), carbonaceous compounds (EC generally higher than OC) and trace elements (Cu, Zn, Mn and occasionally Sn, Sb and Ba) from brake wear (see percentage of species in Tables S2-S6). However, rather dissimilar chemical profiles were found comparing different cities (Figure 4). Although the enrichment in Fe is common to all the cities, the main component of NEX can be either Ca (in BCN-UB), EC (in POR-TR and MLN-UB), OC (in FI-UB), or S (in Athens-SUB). These differences can be due to several factors:

- the proximity to the source: at the traffic site (POR-TR) 28% of the NEX source is made up by EC, which is probably related to brake particles.
- the climatic conditions: Ca is higher in drier regions (BCN-UB and ATH-SUB) due to the enhanced resuspension, when compared to POR-TR and MLN-UB
- the type of materials used for brakes and road pavement (the higher OC in Florence might be due to higher road wear compared to other cities).

Other important differences are the absence of OC in POR-TR (again likely due to the dominance of brake wear particles) and in ATH-SUB, the high abundance of NO_3^- in POR-TR and NH_4^+ in Athens. Note that some elements are absent in some cities since they were not used for the source apportionment study (see Table 2).

The VEX source at all cities is almost totally composed by carbonaceous aerosol (Figure 3), with the sum of OC+EC approximately 90-98% of the mass. The ratio OC/EC varies widely among different cities. The lowest OC/EC value was found at the traffic site of Porto (POR-TR) due to its proximity to the source and the consequent lower proportion of secondary OC. The value varies within 1.8-3.7 at the UB sites, probably linked to the distance from main roads (BCN-UB, MLN-UB and FI-UB). A much higher value (16.4) is observed in ATH-SUB due to the reduced share of diesel vehicles in the local fleet. Besides EC and OC, other components rarely reach 1% of the mass: Zn in MLN-UB, S in BCN-UB and POR-TR due to their relatively higher content in diesel fuel and/or to engine oil anti-wear additive ZDDP. Potassium is present in all unleaded fuels (Spencer et al., 2006) and it is also used as an antifreeze inhibitor and as an additive in some oil types.

The annual mean contributions for VEX and NEX sources and associated errors for each city are showed in Figures 5 and 6. The error estimates were calculated based on the standard error of the coefficients of a multiple regression between the daily PM concentration (independent variable) and the source contributions (dependent variables). As result we obtained the symmetric error for each source contribution (Figure 6).

The sum of VEX and NEX contributions to PM10 varies significantly in absolute terms (3.9-10.8 $\mu g/m^3$) with the maximum found at POR-TR; the fractional contribution to PM10 is within 18-31%. Similarly in PM2.5 absolute annual contributions vary within the range 2.3-9.4 $\mu g/m^3$ but the percentage is quite constant within 14-37% (Figure 5). For the total contribution one should add the

fraction of secondary nitrate attributable to traffic but the lack of linearity between emissions and concentrations and the uncertainty in emission inventorying do not allow for a robust estimate. Although the importance of NEX source has been increasing during the last decade due to the lack of mitigation measures, VEX contribution is still generally higher than NEX. However the difference (in PM10) between the VEX and NEX contribution is not significant at BCN-UB, FI-UB and ATH-SUB sites, which can be generally interpreted as an equal contribution from the two sub-sources. At the TR site (POR-TR) the VEX contribution is significantly higher (by a factor >2).
In PM2.5 the share between VEX and NEX varies considerably depending on the site (Figure 6). At POR-TR, BCN-UB, FI-UB and ATH-SUB the emissions from VEX have higher contribution, while not in MLN-UB. The NEX contribution is significantly lower in PM2.5 due to the coarser size distribution; only in MLN-UB the VEX and NEX contributions in PM2.5 are similar. The daily variation of source contributions at all sites can be seen in Figure S5.

Individual source contributions were also averaged during only days of exceedances of the PM10 daily limit value (50 $\mu g/m^3$), except in BCN-UB where this threshold was never reached and 40 $\mu g/m^3$ was used. During exceedance days (or high pollution days), the sum of VEX and NEX contributions changes in PM10 and PM2.5 respectively from 25 and 21% to 27 and 22% in BCN-UB, from 31 and 31% to 43 and 32% in FI-UB, from 16% and 15% to 19% and 13% in MLN-UB , from 18 and 20% to 7 and 10% in ATH-SUB and from 31 and 37% to 31 and 33% in POR-TR (Table 3).

Secondary processes

Secondary nitrate (SNI) factor reproduces nearly the totality of the mass of ammonium nitrate formed from NOx precursors emitted from traffic, biomass burning and industries. The contribution of road traffic to this factor is unknown. The composition of this factor (Figure 3) is very similar among the different cities, NO_3^- being the main component (28-50%). Nitrate is usually neutralised by ammonium (5-16%) or in the case of ATH-SUB by Na (11%). Another important component is OC representing the condensation of semi-volatile organics on the high specific surface area of the ammonium nitrate particles. EC is also present in significant concentrations (>1%) although not in the case of POR-TR where other primary elements can be observed in this profile (Si, Al, Ca, Fe and K). As previously explained the traffic-related share of secondary nitrate is unknown but in most of sites it is likely to be very important: as an example one should consider that the traffic share of the NO_x emission inventory for the study areas is between 30% and 80%. However the high uncertainty in emission inventory (mostly for the lack of biomass combustion emissions) does not allow drawing quantitative estimates. The secondary nitrate annual average contributions to PM10 range from 2.2 $\mu g/m^3$ in FI-UB, 3.0-3.2 $\mu g/m^3$ in POR-TR, BCN-UB and ATH-SUB, and 11.0 $\mu g/m^3$ in MLN-UB. For PM2.5 the annual contributions are in the range between 0.7 $\mu g/m^3$ (ATH-SUB) to 8.9 $\mu g/m^3$ in MLN-UB. As already mentioned these high nitrate levels in the Po Valley are due to several factors: i) a large urban and industrial agglomeration and associated road traffic; ii) an intensive use of biomass burning in the basin; iii) high NH_3 levels, emitted from agricultural and animal husbandry activities; iv) the peculiar meteorology favouring frequent and marked thermal inversions.

The factor SSO was found at all cities with a rather constant composition, revealing a mainly regional origin of these aerosols across the Mediterranean (Figure 3). The main components are S,

NH_4^+ and OC. EC can be also found at 4-5% concentration in BCN-UB and MLN-UB, indicating a mixing with other (primary) sources. At two sites (POR-TR and MLN-UB), this factor was combined with the heavy oil combustion, thus adding NO_3^-, V and Ni, which in the other cities (BCN-UB, FI-UB and ATH-SUB) appears as an independent source. Other elements that can appear in this source are Si, Na and K, although in concentrations below 1%. SSO aerosols are at all sites in the fine mode (ratio PM2.5/PM10 close to 1), but the variability of contributions across the Mediterranean does not show the same pattern observed for the concentrations of Sulphate. The contributions were progressively increasing from POR-TR (3.3 μg/m^3 in PM2.5), ATH-SUB (3.8 μg/m^3), FI-UB (4.2 μg/m^3) to MLN-UB and BCN-UB (5.7 μg/m^3) (Figure 5). The reason for this higher contribution might be related to the inclusion of some local sources, as suggested by the presence of EC primary combustion particles only at these two sites. The seasonal trend is clear with maxima in the warmer months probably due to the enhanced photochemical activity; this is less clear in MLN-UB where high concentration in fall and winter may be due to aqueous phase formation in the fogs which occur frequently at this time of year (Figure S5). POR-TR registered the highest daily peaks, when the site is under the influence of NW winds, probably due to the emissions from the Porto Refinery, a plant carrying out crude oil industrial processing for the petrochemical industry.

During exceedance days (or high pollution days), the SSO contribution in PM10-PM2.5 always decreases from 27-38% to 19-22% in BCN-UB, from 10-13% to 5-2% in POR-TR, from 21-30% to 6-6% in FI-UB, from 13-19% to 9-11% in MLN-UB, and from 19-32% to 2-5% in ATH-SUB (Table 3).

Marine aerosols

Depending on the geography of each site, sea salt can reach the receptor in a “fresh” or “aged” form, or both. The main chemical difference is the absence of chlorine in the aged sea salt coupled with the presence of the nitrates which means that sodium is in the form of sodium nitrate. Fresh sea salt was identified at POR-TR, FI-UB and ATH-SUB, while aged sea salt was found at MLN-UB, FI-UB and BCN-UB. As shown in Figure 3, the mass fraction of nitrate (μg/μg) is considerably higher in the aged profiles, by one order of magnitude when compared to the fresh profile. In FI-UB, where both fresh and aged factors were found, nitrate is absent in the fresh sea salt and chlorine is absent in the aged factor, which shows also particularly high level of OC indicating the mixing of the aged sea salt with anthropogenic plumes, likely due to the refinery emissions at the coast of Livorno. In all factors the absence of ammonium indicates clearly the neutralisation of nitrate by sodium. Mean contributions of sea salt (Figure 5) in PM10 were revealed to be generally higher (by 25%) than what was found with the chemical speciation (2.5 vs 1.5 μg/m^3 in BCN-UB, 5.5 vs 4.4 μg/m^3 in POR-TR, 1.8 vs 0.6 μg/m^3 in FI-UB, 1.1 vs 0.7 μg/m^3 in MLN-UB, and 1.0 vs 1.6 μg/m^3 in ATH-SUB) due to the involvement of coarse nitrate and water. In PM2.5 the PMF contribution matches with the chemical data (slope = 1, r^2= 0.95). Consequently, the comparison of PMF contributions reflects the same conclusions drawn in the PM speciation section with lower levels of sea salt at the inland Italian cities (FI and MLN) and higher at the Mediterranean coastal sites, with the highest contribution observed at the Atlantic site (POR). Daily source contributions can be seen in Figure S5. During exceedance days (or high pollution days), the sea salt contribution in PM10-

PM2.5 generally decrease from 11-3% to 2-1% in BCN-UB, from 16-4% to 3-0% in POR-TR, from 9-2% to 0-1% in FI-UB, or does not change in MLN-UB and ATH-SUB (Table 3).

Mineral sources

Saharan dust was separated from local dust only at FI-UB, BCN-UB and ATH-SUB (by means of PMF in FI and by the percentile method for BCN and ATH). In MLN-UB and POR-TR the contribution of Saharan dust was estimated as negligible. The chemical profile of Saharan dust (as estimated in FI-UB by PMF) shows a composition very close to the average of the earth's crust, with enrichment factors (EF), calculated with respect to Al using the average continental crust composition reported by (Mason, 1966; Rahn 1976), that are all close to one: 0.99 (Mg), 0.83 (Si), 1.08 (K), 0.92 (Ca), 1.0 (Ti) and 1.1 (Fe) (Figure 3). The annual mean Saharan dust contribution during AIRUSE sampling days was estimated as 0.3 $\mu g/m^3$ (1%) in BCN-UB, 0.7 $\mu g/m^3$ (4%) in FI-UB, and 3.0 $\mu g/m^3$ (14%) in ATH-SUB (Figure 5). This large difference is due to the Southern location of Athens, and the severity of some Saharan dust episodes in the eastern part of the Basin with higher frequency than average, during the period of this study. As mentioned by previous studies, Saharan dust transport occurs in different seasons in western and eastern sides of the Mediterranean (Querol et al., 2009; Pey et al., 2013). Saharan dust inputs in the western side of the Mediterranean are considerably higher between May and October, and in March, when compared to the rest of the year. On the contrary, such inputs are clearly higher between November and May in the eastern part of the Mediterranean. An intermediate outcome is observed for central locations in the Mediterranean, where only slightly higher summer contributions are detected (Pey et al., 2013). For PM2.5 the SAH contribution was estimated only at FI-UB (0.2 $\mu g/m^3$) and ATH-SUB (0.7 $\mu g/m^3$), with PM2.5/PM10 ratio equal to 0.2 in both cases. Concerning PM exceedances, the relative burden of Saharan dust increases during exceedance days only in ATH-SUB, where it is on average the main source of PM10 (52%) and PM2.5 (45%) when the daily limit value of 50 $\mu g/m^3$ is exceeded. No contributions from SAH were found in FI-UB and BCN-UB during days with PM10 above 50 $\mu g/m^3$ and 40 $\mu g/m^3$, respectively.

Besides the long-range transported mineral dust from the Sahara, a significant part of mineral dust was found to be locally emitted in all cities (Local dust, LDU). The ratio SAH/LDU is usually very low: <0.1 in POR-TR and MLN-UB, 0.1 in BCN-UB and 0.3 in FI-UB, indicating that at these sites Saharan dust is 0-23% of measured mineral dust, with the rest emitted by human activities or of local origin. Only in ATH-SUB the SAH contribution was higher (ratio SAH/LDU=1.4) than the local dust due both to the geographical position of Athens and the suburban location of the measurement site (i.e. lower anthropogenic contribution than at UB sites). The chemical profile of LDU is the one shown in Figure 3 (the MIN profile is used). Although the major components are similar at all sites (Si, Al, Ca, Fe, OC and K), some differences can be observed. The highest ratio Ca/Al is found in FI-UB (6.3) due to the clear PMF separation from SAH contribution (ratio Ca/Al=0.4, similarly to earth crust). The other cities show Ca/Al ratios in the mineral dust factors varying from 0.5 (POR-TR) to 2.2 (BCN-UB), which is influenced by the SAH contribution as well as the local geology and share of Ca-rich local emissions. The ratio Si/Al varies within 2.0 and 3.8. The ratio OC/Ca is generally well above the stoichiometric CC/Ca ratio in calcite (0.3) revealing additional sources of organic carbon such as biogenic OC and/or road dust, mostly in MLN-UB, where the complex atmospheric dynamics impede the separation of sources. Other common

components of LDU are NO_3^- (except in POR-TR), S likely from gypsum, Cu, Zn and Ba, suggesting possible interference from road dust. LDU contributions to PM10 range within 8-12% at SUB and UB sites (2.4-3.3 μg/m^3) and increase to 6.3 μg/m^3 (18%) at the TR site, revealing a contribution from road dust resuspension. In PM2.5 the SUB-UB range was 0.3-1.5 μg/m^3 (2-7%) and 3.8 μg/m^3 (15%) at the TR site. The relative contribution (%) does not increase during exceedances days, with the exception of POR-TR, where it rises to 28% and 20% for PM10 and PM2.5, respectively. The daily variation of LDU contributions shows generally higher values from spring to autumn at all cities (Figure S5). Above the background contributions, sporadic peaks are also found, mostly at POR-TR, probably related to road dust emissions, not well completely included in the NEX factor.

Heavy oil combustion

As already mentioned, the contribution of heavy oil combustion was separated only at the cities nearest to the Mediterranean shipping routes (BCN, FI and ATH) in spite of the fact that V and Ni concentrations in POR-TR were twice as high as in FI-UB. In POR-TR and MLN-UB, the HOC source is mixed with the SSO in the combined source HOS. HOC particles are commonly composed by EC, OC and S explaining the high variance of V and Ni. The difference between AIRUSE sites concerns only specific trace elements such as Zn, Sn, Ba (in BCN-UB), Ba and Se (in FI-UB), Sr and Sb (in ATH-SUB), although only a small amount of variance of these elements is explained by HOC (Tables S2-S6). The annual contribution of HOC is practically the same in BCN-UB, FI-UB and ATH-SUB (0.8-1.0 μg/m^3 in PM10 and 0.7-0.8 μg/m^3 in PM2.5). The contribution in POR-TR and MLN-UB could not be separated from the composite HOS. The daily variation of HOC contributions, as estimated by PMF is shown in Figure S5. In FI-UB and BCN-UB higher contributions are observed in summer due to the higher air circulation, which favours their transport and distribution across the regional area, while in ATH-SUB no clear seasonal trend is observed for HOC probably because of the variety of the sources that may contribute to this factor (residential heating and shipping). During exceedance days (or high pollution days), the HOC contribution in PM10-PM2.5 does not change significantly.

Industrial emissions

The impact of industrial emissions was identified in only three cities: BCN-UB, POR-TR and MLN-UB. Florence and Athens are in fact the less industrialised cities among the AIRUSE consortium. In the three industrialised cities, OC and Fe are commonly present as main components (Figure 3). Besides OC and Fe, in BCN-UB and POR-TR the presence of Zn, Pb, S, Cu, Cd, Sb and Mn indicate high temperature metal processing, pointing at the smelters located SW of BCN-UB and East of POR-TR. In MLN-UB the industrial source presents a different chemical profile with NO_3^-, EC, Ca, Cl as main components (together with OC and Fe) and a high variance of Cr, Ni, Cu and Mn explained, suggesting a more mixed origin, including metallurgy and also construction activities (Tables S2-S6). The impact of industrial emissions upon PM10 and PM2.5 is similarly low at MLN, POR and BCN, ranging within 1.2-3.3 μg/m^3 as annual means and with a PM2.5/PM10 ratio close to 1. No typical seasonal trend is observable at any site (Figure S5). The contribution was rather constant throughout the year (around 1 μg/m^3 daily) in MLN-UB and BCN-UB, while elevated peaks (up to 13 μg/m^3 as a daily mean) are registered in POR-TR, mostly in the warmer months. During exceedance days (or high pollution days), the IND contribution in PM10-

PM2.5 slightly increases from 11-12% to 17-19% in BCN-UB, and decreases from 4-5% to 2-1% in POR-TR, and from 9-5% to 4-3% in MLN-UB (Table 3).

Biomass burning

As previously shown, concentrations of levoglucosan varied by over one order of magnitude among the AIRUSE cities, indicating very contrasting scenarios across the Mediterranean for emissions from biomass burning. Similarly, the PMF identified a biomass burning source only in four of the five cities due to the low levels of levoglucosan in BCN-UB (20 ng/m^3 as annual mean). In all other cities, levoglucosan is the main tracer in the chemical profile of the biomass burning source identified by PMF (except in ATH-SUB, where levoglucosan was not used as input species for PMF due to the high S/N ratio). Levoglucosan represents 4-8% of PM mass in biomass burning factor profile; OC and EC are the major components in the BB profile (12-65% and 4-14%, respectively). In spite of these quite large ranges, the OC/EC ratio can be used as a more robust diagnostic of BB composition. The OC/EC ratio in BB aerosols varies from 2.6 (ATH-SUB), 2.9 (POR-TR), 4.6 (MLN-UB) to 6.1 (FI-UB) which may be explained by a higher proportion of secondary organic aerosols in MLN-UB and FI-UB or by different wood types and combustion appliances. Also K (probably the soluble fraction) tracks BB aerosols, representing 2-4% of the mass. Other components can be observed, although more sporadically, such as Cl, S, Zn, Pb, NH_4^+ and NO_3^- (Figures 3 and Tables S2-S6). BB contributions reproduce quite well the gradients found for levoglucosan among the AIRUSE cities. Although levoglucosan has been detected in some samples from BCN, biomass burning could not be assigned as a significant contributor to PM. In the other cities, an annual mean of 1.2-1.4 μg/m^3 (7-10%) is estimated in ATH-SUB, 2.9-2.8 μg/m^3 (15-20%) in FI-UB, 4.2-4.4 μg/m^3 (12-17%) in POR-TR, up to 7.3-5.1 μg/m^3 (17%) in MLN-UB. Therefore, this reveals quite a contrasting impact of BB emissions across the Mediterranean depending on the type of fuel and combustion device used in each region for residential heating. Differently from other cities, Barcelona is well supplied with natural gas for residential heating; Florence is also well supplied with natural gas but in the suburbs on the hill there are commonly chimneys. Even in Milan the use of natural gas for heating is very extensive, however, also due to the current economic crisis, many citizens are equipped with small pellet stoves. In ATH the BB source is also associated with tracers of waste combustion, such as As, Cd, Sb and Pb, with explained variance ranging between 12% and 72%, as citizens of Athens have turned to alternative heating fuels, such as wood, due to the economic crisis and the increased prices of diesel oil, which has been the regular means of residential heating in Greece. In many cases, treated wood or even combustible wastes are now used as fuel. As previously shown for the traffic source, another factor identified by PMF was secondary nitrate (SNI). Although in urban environments nitrate mainly arises from NO_x from traffic, a substantial fraction can also be derived from biomass burning emissions. Therefore for each city, the corresponding share of NO_x due to biomass burning can be applied also to SNI. Based on this approach, percentages of 16 and 13 were adopted in POR-TR and MLN-UB, respectively, to account for SNI from biomass burning. In FI-UB, on the basis of the emission inventory, about 10% of NO_x emissions are due to domestic heating, with only 2% attributable to stoves and chimneys (http://servizi2.regione.toscana.it/aria/); it is however suspected that these data underestimate the contribution of domestic heating BB to NO_x. Thus, in POR-TR, the total contribution from BB was estimated to be 4.7 μg/m^3 (13% of PM10) and 4.6 μg/m^3 (18%

of PM2.5). In MLN-UB, the total contribution from BB represented 8.7 μg/m^3 in PM10 (23%) and 6.3 μg/m^3 in PM2.5 (21%).

The impact of BB emissions is especially high in the winter months (Figure S5), due to the generalised use of wood for residential heating (Gonçalves et al., 2012). The contribution of BB to PM in POR-TR was also higher in September. Several wildfires were registered in the Porto district in this particularly hot and dry month. In MLN-UB the stagnant conditions and reduced boundary layer height induced by the typical meteorology of the Po Valley also enhance BB contributions during winter months. The relative contribution from biomass burning to PM10 and PM2.5 generally increases on exceedance days in POR-TR, MLN-UB and FI-UB. The percentages increase in fact from 23-21% to 35-26% in MLN-UB, from 13-18% to 25-36% (POR-TR), from 15-20% to 30-32% (FI-UB). Conversely, in ATH-SUB, during exceedances days the contribution from BB is substantially reduced (from 7-10% to 1-2%, Table 3). This is again due to exceedances in Athens being caused by African dust intrusions and the relative suppression of other source contribution during exceedance days.

Recent research attention has been focused on the importance of other sources/process contributing to the non-fossil OC in urban ambient air, namely food cooking (Crippa et al. 2013, Allan et al., 2010; Mohr et al., 2012), and enhanced biogenic secondary aerosols (Hoyle et al., 2011; Kroll et al., 2006). The quantification of these two sources/processes require the use of a combination of measurement techniques: Aerosol Mass Spectrometer (AMS) and off-line radiocarbon analysis on PM filters, which could not be performed within AIRUSE. For example, in summer in Barcelona cooking was estimated to be responsible of 17% of organic aerosols (OA being 60% ofPM1) (Minguillón et al., 2015), while in Athens COA was not found as a separate source, but mixed with the traffic-related factor, contributing 17% of OA (Kostenidou et al., 2014). The influence of road traffic emissions such as NOx on the formation of biogenic secondary aerosols (Hoyle et al., 2011) has been observed in Barcelona, where an increase of non-fossil secondary organic aerosol was registered when comparing a period with low traffic emissions with a period with high traffic emissions, supported by the increase of individual organic compounds such as poly-acids (malic acid, 3-hydroglutaric acid, MBTCA and 2-methylglyceric acid) (Minguillón et al., 2015).

4.Conclusions

Based on the simultaneous chemical characterisation of PM10 and PM2.5 samples collected every third day across 12 months at five Southern European cities important differences were observed. Thus, in FI-UB, MLN-UB and POR-TR**,** OM+EC was the main PM10 constituent, accounting for 57, 45 and 37% of the PM10 load and 69, 45 and 48 of the PM2.5. However, at BCN-UB and ATH-SUB these PM components were still dominant, but made up only 27 and 36% of PM10 and 30 and 45% of PM2.5.

The PM fraction accounted by secondary inorganic aerosols (sulphate, nitrate and ammonium) showed also significant variations with a load of 18-20% of PM10 for FI-UB and BCN-UB, 30% for ATH-SUB and 35% in MLN-UB, and 21-22% of PM2.5 for FI-UB and BCN-UB, 33% in MLN-UB and 37% for ATH-SUB. For the POR-TR site the SIA percentage was reduced due to the increase of contributions from OM+EC (mostly from exhaust emissions) and mineral dust (mostly from road dust), and made up 15% of PM10 and PM2.5.

Mineral dust was one of the main PM10 components at all sites ranging from 10 (MLN-UB) to 21% (ATH-SUB) of the PM10 load. In PM2.5, as expected from the coarser mode of occurrence of mineral dust, the contribution was reduced down to 4 (FI) – 10% (ATH) in all cases.
The sea salt contribution reached the maximum at the Atlantic site, 13% of PM10 and 5% of PM2.5 in POR, followed by the other two Mediterranean coastal sites, BCN and ATH (7 and 8 % of PM10 and 3 and 2 % of PM2.5); the minimum sea salt contributions were recorded in the inland Italian cities, MLN and FI (2-3% of PM10 and 1% of PM2.5).

The sum of vehicle exhaust and vehicle non-exhaust emissions is unequivocally the most important source of PM10 (18-31% at all sites, except in MLN-UB where SNI and SSO dominate the mass), while for PM2.5 it is clearly the largest source for POR-TR (37%), the second one at BCN-UB, FI-UB and ATH-SUB after Secondary sulphate and organics (which likely receives significant transboundary contribution). In PM2.5 MLN-UB Secondary nitrate is the main contributor although it does not identify one specific source.
Another important "source" of PM10 (19-27%) is Secondary sulphate and organics at BCN-UB, FI-UB and ATH-SUB, while this only represents 13% of PM10 in MLN-UB and 10% of PM10 in POR-TR. The relative importance of Secondary sulphate and organics is higher in PM2.5 (19-38% at SUB and UB sites and 13% in POR-TR). The contributions (in PM2.5) progressively increase from POR-TR (3.3 $\mu g/m^3$), ATH-SUB (3.8 $\mu g/m^3$), FI-UB (4.2 $\mu g/m^3$) to MLN-UB and BCN-UB (5.6-5.7 $\mu g/m^3$).
Another important source of PM10 is Biomass burning (13% in POR-TR, 15% in FI-UB, and 23% in MLN-UB), although it is only 7% in ATH-SUB and negligible in BCN-UB. In PM2.5, BB is the second most important source in MLN-UB (21%) and in POR-TR (18%), the third in FI-UB (20%) and ATH-SUB (10%), but again negligible (<2%) in BCN-UB. This large discrepancy among cities is mostly due to the degree of penetration of wood (and its derivatives) as fuel for residential heating. In Barcelona natural gas is very well supplied across the city and used as fuel in 96% of homes, while, in other cities, PM levels increase on an annual basis by 1-6 $\mu g/m^3$ due to this source.
Other significant anthropogenic sources are:
- Local dust, 8-12% of PM10 at SUB and UB sites and 18% at the TR site, revealing a contribution from road dust resuspension. In PM2.5 percentages decrease to 2-7% at SUB-UB sites and 15% at the TR site.
- Industry, mainly metallurgy contributing 4-8% of PM10 (5-9% in PM2.5), but only at BCN-UB, POR-TR and MLN-UB. No clear impact of industrial emissions was found in FI-UB and ATH-SUB.
- Natural contributions consist of Sea salt (16% of PM10 in POR-TR but only 2-11% in the other cities) and Saharan dust (14% in ATH-SUB) but less than 4% in the other cities.
- Other sources of non-fossil OC, such as food cooking and the formation of enhanced biogenic secondary organic aerosol could not be separated due to the lack of specific techniques.
During high pollution days, the largest specific source (i.e. excluding SSO and SNI) of PM10 and PM2.5 are: VEX+NEX in BCN-UB (27-22%) and POR-TR (31-33%), BB in FI-UB (30-33%) and MLN-UB (35-26%) and Saharan dust in ATH-SUB (52-45%). During those days, there are also quite important Industrial contributions in BCN-UB (17-18%) and Local dust in POR-TR (28-20%).

Acknowledgments

This work was funded by the AIRUSE LIFE+ EU project. Fulvio Amato is beneficiary of the Juan de la Cierva postdoctoral grant (JCI-2012-13473) from the Spanish Ministry of Economy and Competitiveness. Danilo Custódio acknowledges the doctoral fellowship SFRH/BD/76283/2011 from the Portuguese Science Foundation.

References

Aiken, A.C., Decarlo, P.F., Kroll, J.H., Worsnop, D.R., Huffman, J.A., Docherty, K.S., Ulbrich, I.M., Mohr, C., Kimmel, J.R., Sueper, D., Sun, Y., Zhang, Q., Trimborn, A., Northway, M., Ziemann, P.J., Canagaratna, M.R., Onasch, T.B., Alfarra, M.R., Prevot, A.S.H., Dommen, J., Duplissy, J., Metzger, A., Baltensperger, U., Jimenez, J.L. O/C and OM/OC ratios of primary, secondary, and ambient organic aerosols with high-resolution time-of-flight aerosol mass spectrometry (2008) Environmental Science and Technology, 42 (12), pp. 4478-4485.

Alastuey, A., Querol, X., Castillo, S., Escudero, M., Avila, A., Cuevas, E., Torres, C., Romero, P.-M., Exposito, F., García, O., Diaz, J.P., Van Dingenen, R., Putaud, J.P.: Characterisation of TSP and PM2.5 at Izaña and Sta. Cruz de Tenerife (Canary Islands, Spain) during a Saharan Dust Episode (July 2002),Atmos. Environ., 39 (26), 4715-4728, 2005.

Allan, J. D., Williams, P. I., Morgan, W. T., Martin, C. L., Flynn, M. J., Lee, J., Nemitz, E., Phillips, G. J., Gallagher, M. W., and Coe, H.: Contributions from transport, solid fuel burning and cooking to primary organic aerosols in two UK cities, Atmos. Chem. Phys., 10, 647–668 2010

Amato, F., Pandolfi, M., Escrig, A., Querol, X., Alastuey, A., Pey, J., Perez, N., Hopke, P.K.: Quantifying road dust resuspension in urban environment by Multilinear Engine: A comparison with PMF2.Atmos. Environ., 43, 2770–2780, 2009.

Calzolai G., Nava S., Lucarelli F., Chiari M., Giannoni M., Becagli S., Traversi R., Marconi M., Frosini D., Severi M., Udisti R., di Sarra A., Pace G., Meloni D., Bommarito C., Monteleone F., Anello F., Sferlazzo D. M., "Characterization of PM10 sources in the central Mediterranean", Atmos. Chem. Phys. 15 (2015), 13939-13955

Council Directive 2008/50/EC of the European Parliament and of the Council of 21 May 2008 on ambient air quality and cleaner air for Europe OJ L 152, 11.6.2008, pp. 1–44.

Crippa, M., DeCarlo, P. F., Slowik, J. G., Mohr, C., Heringa, M. F., Chirico, R., Poulain, L., Freutel, F., Sciare, J., Cozic, J., Di Marco, C. F., Elsasser, M., José, N., Marchand, N., Abidi, E., Wiedensohler, A., Drewnick, F., Schneider, J., Borrmann, S., Nemitz, E., Zimmermann, R., Jaffrezo, J.-L., Prévôt, A. S. H., and Baltensperger, U.: Wintertime aerosol chemical composition and source apportionment of the organic fraction in the metropolitan area of Paris, Atmos. Chem. Phys., 13, 961–981 2013

Draxler, R.R. and Rolph G.D., 2003. HYSPLIT (HYbrid Single-Particle Lagrangian Integrated Trajectory) Model access via NOAA ARL READY Website (http://www.arl.noaa.gov/ready/hysplit4.html). NOAA Air Resources Laboratory, Silver Spring, MD.

Eeftens, M., Beelen, R., De Hoogh, K., Bellander, T., Cesaroni, G., Cirach, M., Declercq, C., Dedele, A., Dons, E., De Nazelle, A., Dimakopoulou, K., Eriksen, K., Falq, G., Fischer, P., Galassi, C., Gražulevičiene, R., Heinrich, J., Hoffmann, B., Jerrett, M., Keidel, D., Korek, M., Lanki, T., Lindley, S., Madsen, C., Mölter, A., Nádor, G., Nieuwenhuijsen, M., Nonnemacher, M., Pedeli, X., Raaschou-Nielsen, O., Patelarou, E., Quass, U., Ranzi, A., Schindler, C., Stempfelet, M., Stephanou, E., Sugiri, D., Tsai, M.-Y., Yli-Tuomi, T., Varró, M.J., Vienneau, D., Klot, S.V., Wolf, K., Brunekreef, B., Hoek, G.: Development of land use regression models for PM2.5, PM 2.5 absorbance, PM10 and PMcoarse in 20

European study areas; Results of the ESCAPE project, Envir. Sci. Tech., 46 (20), 11195-11205, 2012.

Fine, P.M., Cass, G.R., Simoneit, B.R.T.:. Chemical characterization of fine particle emissions from fireplace combustion of woods grown in the northeastern United States, Envir. Sci. Tech. 35, 13, 2665-2675, 2001.

Gietl, J.K., Lawrence, R., Thorpe, A.J., Harrison, R.M.: Identification of brake wear particles and derivation of a quantitative tracer for brake dust at a major road. Atmos. Envir. 44, 141-146, 2010.

Gonçalves, C., Alves, C., Pio, C.: Inventory of fine particulate organic compound emissions from residential combustion in Portugal, Atmos. Envir., 50, 297-306, 2012.

Gonçalves, C., Alves, C., Evtyugina, M., Mirante, F., Pio, C., Caseiro, A., Schmidl, C., Bauer, H., Carvalho, F.: Characterisation of PM10 emissions from wood stove combustion of common woods grown in Portugal, Atmos. Environ, 44, 4474-4480, 2010.

Hennigan, C. J., Izumi, J., Sullivan, A. P., Weber, R. J., and Nenes, A.: A critical evaluation of proxy methods used to estimate the acidity of atmospheric particles, Atmos. Chem. Phys., 15, 2775-2790, doi:10.5194/acp-15-2775-2015, 2015.

Henry, R.C., Hidy, G.M. Multivariate analysis of particulate sulphate and other air quality variables by principal components-Part I: Annual data from Los Angeles and New York, Atmos. Environ. (1967), 13 (11), 1581-1596, 1979.

Hodzic, A., Madronich, S., Bohn, B., Massie, S., Menut, L., Wiedinmyer, C.: Wildfire particulate matter in Europe during summer 2003: meso-scale modeling of smoke emissions, transport and radiative effects, Atmos. Chem. Phys., 7, 4043–4064, 2007.

Hoyle, C.R., Boy, M., Donahue, N.M., Fry, J.L., Glasius, M., Guenther, A., Hallar, A.G., Huff Hartz, K., Petters, M.D., Petäjä, T., Rosenoern, T., Sullivan, A.P.: A review of the anthropogenic influence on biogenic secondary organic aerosol, Atmos. Chem. Phys., 11, 321–343, 2011.Karanasiou, A., Querol, X., Alastuey, A., Perez, N., Pey, J., Perrino, C., Berti, G., Gandini, M., Poluzzi, V., Ferrari, S., de la Rosa, J., Diaz, J., Pascal, M., Samoli, E., Kelesis, A., Sunyer, J., Alessandrini, E., Stafoggia, M., Forastiere, F. and the Med Particles Study Group: Particulate matter and gaseous pollutants in the Mediterranean Basin: Results from the Med-Particles project. Sci, Total Environ., 488–489, 297-315, 2014.

Kostenidou, E., Florou, K., Kaltsonoudis, C., Tsiflikiotou, M., Vratolis, S., Eleftheriadis, K., and Pandis, S. N.: Sources and chemical characterization of organic aerosol during the summer in the eastern Mediterranean, Atmos. Chem. Phys. Discuss., 15, 3455-3491, 2015.

Kroll, J. H., Ng, N. L., Murphy, S. M., Flagan, R. C., Seinfeld, J. H.. Secondary organic aerosol formation from isoprene photooxidation, Environ. Sci. Technol., 40, 1869–1877, 2006.

Mason, B., 1966. Principles of Geochemistry, 3rd ed. Wiley, New York

Lianou, M., Chalbot, M.-C., Kavouras, I.G., Kotronarou, A., Karakatsani, A., Analytis, A., Katsouyanni, K., Puustinen, A., Hameri, K., Vallius, M., Pekkanen, J., Meddings, C., Harrison, R.M., Ayres, J.G., ten Brick, H., Kos, G., Meliefste, K., de Hartog, J., Hoek, G: Temporal variations of atmospheric aerosol in four European urban areas, Environ. Sci. Pollut. R., 18, 1202-1212, 2011..

Lucarelli, F., Calzolai, G., Chiari, M., Giannoni, M., Mochi, D., Nava, S., Carraresi, L.: The upgraded external-beam PIXE/PIGE set-up at LABEC for very fast measurements on aerosol samples, Nucl. Instrum. Meth. Phys. Res. B 318, 55–59, 2014

Minguillón, M.C., Perron, N., Querol, X., Szidat, S., Fahrni, S.M., Alastuey, A., Jimenez, J.L., Mohr, C., Ortega, A.M., Day, D.A., Lanz, V.A., Wacker, L., Reche, C., Cusack, M., Amato, F., Kiss, G., Hoffer, A., Decesari, S., Moretti, F., Hillamo, R., Teinilä, K., Seco, R., Peñuelas, J., Metzger, A., Schallhart, S., Müller, M., Hansel, A., Burkhart, J.F., Baltensperger, U., Prévót, A.S.H. Fossil versus contemporary sources of fine elemental and

organic carbonaceous particulate matter during the DAURE campaign in Northeast Spain (2011) Atmospheric Chemistry and Physics, 11 (23), pp. 12067-12084.

M. C. Minguillón, N. Pérez, N. Marchand, A. Bertrand, B. Temime-Roussel, K. Agrios, S. Szidat, B. L. van Drooge, A. Sylvestre, A. Alastuey, C. Reche, A. Ripoll, E. Marco, J. O. Grimalt and X. Querol, Secondary organic aerosol origin in an urban environment. Influence of biogenic and fuel combustion precursors. Faraday Discuss., 2015, DOI: 10.1039/C5FD00182J

Mohr, C., DeCarlo, P.F., Heringa, M.F., Chirico, R., Slowik, J.G., Richter, R., Reche, C., Alastuey, A., Querol, X., Seco, R., Peñuelas, J., Jiḿenez, J.L., Crippa, M., Zimmermann, R., Baltensperger, U., Prévôt, A.S.H.: Identification and quantification of organic aerosol from cooking and other sources in Barcelona using aerosol mass spectrometer data , Atmos. Chem. Phys., 12 (4), 1649-1665, 2012.

Nava, S., Lucarelli F., Amato F., Becagli S., Calzolai G., Chiari M., Giannoni M., Traversi R., Udisti R.: Biomass burning contributions estimated by synergistic coupling of daily and hourly aerosol composition records, Sci. Total Environ., 511, 11-20

Nava S., Becagli S., Calzolai G., Chiari M., Lucarelli F., Prati P., Traversi R., Udisti R., Valli G., Vecchi R., "Saharan dust impact in central Italy: An overview on three years elemental data records", Atm. Env. 60 (2012), 444-452

Paatero, P.. The multilinear engine—a table-driven least squares program for solving multilinear problems, including the n-way parallel factor analysis model, J. Comput. Graph. Stat., 8, 854–888, 1999.

Paatero, P. and Hopke, P.K.: Rotational tools for factor analytic models implemented by using the multilinear engine, Chemometrics, 23 (2), 91-100, 2008.

Paatero, P., and Hopke, P.K.: Discarding or downweighting high-noise variables in factor analytic models, Anal. Chim. Acta, 490 (1-2), 25, 277-289, 2003.

Paatero, P. and Tapper, U.: Positive matrix factorization: A non-negative factor model with optimal utilization of error estimates of data values, Environmetrics, 5, 111-126, 1994.

Pikridas, M., Tasoglou, A., Florou, K., Pandis, S.N.: Characterization of the origin of fine particulate matter in a medium size urban area in the Mediterranean, Atmos. Environ., 80, 264-274, 2013. Pio, C.A., Ramos, M.M., Duarte, A.C.: Atmospheric aerosol and soiling of external surfaces in an urban environment, Atmos. Environ., 32, 1979-1989, 1998..

Pio, C., Cerqueira, M., Harrison, R.M., Nunes, T., Mirante, F., Alves, C., Oliveira, C., Sanchez de la Campa, A., Artiñano, B., Matos, M.: OC/EC Ratio Observations in Europe: Re-thinking the approach for apportionment between primary and secondary organic carbon, Atmos. Environ. 45, 6121-6132, 2011.

Pio, C.A., Castro, L. M., and Ramos, M. O.: Differentiated determination of organic and elemental carbon in atmospheric aerosol particles by a thermal-optical method, in: Proceedings of the Sixth European Symposium: Physico-Chemical Behaviour of Atmospheric Pollutants, edited by: Angeletti, G. and Restelli, G., Report EUR 15609/2 EN, European Commission, 706–711, 1994.

Polissar, A.V., Hopke, P.K., Paatero, P., Malm, W.C., Sisler, J.F. Atmospheric aerosol over Alaska 2. Elemental composition and sources, J. Geophys. Res- Atmos, 103 (D15), 98JD01212 , 19045-19057, 1998.

Puxbaum, H., Caseiro, A., Sánchez-Ochoa, A., Kasper-Giebl, A., Claeys, M., Gelencsér, A., Legrand, M., Preunkert, S., Pio, C.A.: Levoglucosan levels at background sites in Europe for assessing the impact of biomass combustion on the European aerosol background. J. Geophys. Res- Atmos, 112, 23, D23S05, 2007.

Querol, X., Alastuey, A., Rodríguez, S., Plana, F., Mantilla, E., Ruiz C.R.: Monitoring of PM10 and PM2.5 around primary particulate anthropogenic emission sources, Atmos. Environ. 35, 845–858, 2001.

Querol, X., Alastuey, A., Ruiz, C.R., Artiñano, B., Hansson, H.C., Harrison, R.M., Buringh, E., Ten Brink, H.M., Lutz, M., Bruckmann, P., Straehl, P., Schneider, J.: Speciation and origin of PM10 and PM2.5 in selected European cities, Atmos. Environ., 38, 6547-6555, 2004.

Querol, X., Alastuey, A., Viana, M., Moreno, T., Reche, C., Minguillón, M.C., Ripoll, A., Pandolfi, M., Amato, F., Karanasiou, A., Pérez, N., Pey, J., Cusack, M., Vázquez, R., Plana, F., Dall'Osto, M., De La Rosa, J., Sánchez De La Campa, A., Fernández-Camacho, R., Rodríguez, S., Pio, C., Alados-Arboledas, L., Titos, G., Artíñano, B., Salvador, P., García Dos Santos, S., Fernández Patier, R.:Variability of carbonaceous aerosols in remote, rural, urban and industrial environments in Spain: Implications for air quality policy, Atmos. Chem. Phys., 13 (13), 6185-6206, 2013..

Querol, X., Pey, J., Pandolfi, M., Alastuey, A., Cusack, M., Moreno,T., Viana, M., Mihalopoulos, N., Kallos, G., and Kleanthous, S.: African dust contributions to mean ambient PM10 levels across the Mediterranean Basin, Atmos. Environ., 43, 4266–4277, 2009.

Rahn, K.A.:. Silicon and aluminum in atmospheric aerosols: crust-air fractionation? Atmos. Environ., 10, 597-601, 1976

SEC, 2011.208 final. Secretary-General of the European Commission. Commission Staff Working Paper establishing guidelines for demonstration and subtraction of exceedances attributable to natural sources under the Directive 2008/50/EC on ambient air quality and cleaner air for Europe. Brussels, 15.02.2011.

Simoneit, B.R.T., Schauer, J.J., Nolte, C.G., Oros, D.R., Elias, V.O., Fraser, M.P., Rogge, W.F., Cass, G.R.: Levoglucosan, a tracer for cellulose in biomass burning and atmospheric particles. Atmos. Environ. 33, 2, 173-182, 1999..

Spencer, M.T., Shields, L.G., Sodeman, D.A., Toner, S.M., Prather, K.A.: Comparison of oil and fuel particle chemical signatures with particle emissions from heavy and light duty vehicles. Atmos Environ 40: 5224–5235, 2006.

Thurston, G.D. and Spengler, J.D.: A quantitative assessment of source contributions to inhalable particulate matter pollution in metropolitan Boston, Atmos. Environ. (1967), 19, (1), 9-25, 1985.

Traversi, R., Becagli, S., Calzolai, G., Chiari, M., Giannoni, M., Lucarelli, F., Nava, S., Rugi, F., Severi, M., Udisti, R.: A comparison between PIXE and ICP-AES measurements of metals in aerosol particulate collected in urban and marine sites in Italy, Nucl. Instr. & Meth. B 318 130-134, 2014.

Turpin, B. J. and Huntzicker, J. J.: Identification of secondary organic aerosol episodes and quantisation of primary and secondary organic aerosol concentrations during SCAQS, Atmos. Environ., 29, 3527–3544, 1995.

US EPA Positive Matrix Factorization (PMF) 5.0 Fundamentals and User Guide. EPA/600/R-14/108 April 2014 www.epa.gov

Watson, J.G., Cooper, J.A., Huntzicker J.J., The effective variance weighting for least squares calculations applied to the mass balance receptor model Atmospheric Environment (1967), 18, (7),1347-1355, 1984.

WHO, 2012. Health effects of black carbon. ISBN: 978 92 890 0265 3. See at: http://www.euro.who.int/__data/assets/pdf_file/0004/162535/e96541.pdf

Table 1. Mean PM and component concentrations for the study period at the five AIRUSE cities. NA: not available

	PM10					PM2.5				
ng/m^3	BCN-UB	POR-TR	FI-UB	MLN-UB	ATH-SUB	BCN-UB	POR-TR	FI-UB	MLN-UB	ATH-SUB
PM	22526	34520	18896	38074	19782	15001	26680	13213	30129	11003
p90.4	33578	52869	31094	65644	30946					
OM	4959	7625	9634	15354	5556	4400	7783	8162	11741	4631
TC	3863	10969	6440	10357	3684	3444	11288	5468	8307	3048
EC	1108	4814	1088	1827	416	1000	5006	934	1784	324
OC	2755	6155	5352	8530	3268	2444	6282	4534	6523	2724
CO_3^{2-}	151	35	144	29	34	NA	NA	NA	NA	NA
SO_4^{2-}	1985	2470	1737	3001	3651	1685	2000	1542	1934	2888
NO_3^-	1990	1954	1184	6009	1164	922	1198	639	5675	173

NH_4^+	604	703	496	3327	1013	709	658	548	2201	943
Levoglucosan	NA	NA	NA	NA	NA	20	387	255	274	37
K	176	429	250	373	251	87	343	172	303	115
S	751	890	780	1089	1255	581	782	698	1071	911
Cl	599	2284	254	341	617	178	690	22	272	41
Na	697	1488	375	190	670	163	440	59	178	112
Mg	155	283	116	113	210	40	82	17	21	35
Al	225	444	194	282	400	66	226	39	149	90
Si	533	912	569	872	994	156	475	126	325	234
Ca	618	336	619	640	778	143	166	104	237	175
Fe	477	841	446	1141	419	146	374	88	317	112
Cu	19.3	32.1	22.3	61.9	6.2	6.9	15.6	4.7	32.6	2.2
Zn	63.8	103.2	18.7	82.6	18.0	45.0	90.7	10.3	56.2	9.9
Ba	11.1	35.6	14.9	59.6	16.1	4.4	15.8	4.7	52.3	6.9
Sn	4.6	8.1	NA	34.0	1.5	2.2	4.7	NA	32.3	1.0
Sb	2.6	5.2	NA	21.2	0.8	1.1	5.1	NA	20.7	0.5
Ni	1.7	2.8	1.4	5.3	2.6	1.3	2.4	1.0	4.6	1.5
V	4.5	4.6	2.1	2.3	4.0	3.7	3.1	1.7	2.6	2.7
Cr	3.0	4.6	3.2	4.7	2.5	1.3	2.0	0.8	2.1	2.0
Mo	9.3	4.1	1.7	NA	1.8	9.7	1.7	1.5	NA	1.7
Pb	7.0	15.0	4.3	18.6	4.2	5.4	13.3	3.7	15.2	2.7
Cd	0.2	0.2	0.2	NA	0.1	0.1	0.3	0.2	NA	0.1
Co	0.1	0.1	NA	NA	0.1	0.1	0.2	NA	NA	0.1
As	0.4	1.6	0.5	NA	0.6	0.3	0.7	0.4	NA	0.4
Se	0.3	1.0	0.6	NA	0.5	0.2	0.4	0.5	NA	0.3
Ge	0.2	0.1	NA	NA	0.6	0.2	0.1	NA	NA	0.6
W	0.4	0.3	NA	NA	0.6	0.2	0.5	NA	NA	0.6
Bi	0.4	0.3	NA	NA	0.1	0.2	0.2	NA	NA	0.1
Br	NA	10.9	4.4	19.8	5.7	NA	7.6	3.6	10.3	3.4
P	16.0	24.2	9.5	28.0	9.2	6.5	11.0	3.5	NA	6.8
Ti	16.3	25.5	13.7	30.2	24.7	4.9	14.5	3.5	14.3	8.2
Mn	9.9	14.3	7.1	16.3	7.1	4.6	8.8	2.1	8.5	2.2
Rb	0.4	5.6	1.7	1.6	1.7	0.2	2.7	0.7	0.9	0.8
Sr	2.1	3.6	2.1	13.0	3.1	0.6	1.1	0.8	13.5	1.0
Y	0.2	6.2	0.7	NA	0.7	0.2	1.7	0.7	NA	0.7
Zr	6.7	5.9	2.2	NA	1.7	5.5	2.3	0.8	NA	1.1
Li	0.2	0.7	NA	NA	0.3	0.1	0.5	NA	NA	0.1
Nb	0.4	0.5	NA	NA	0.5	0.2	0.5	NA	NA	0.3
Ga	0.1	0.2	NA	NA	0.2	0.1	0.2	NA	NA	0.1
Th	0.1	0.01	NA	NA	0.2	0.1	0.1	NA	NA	0.2
La	0.2	0.3	0.5	NA	0.3	0.1	0.2	0.3	NA	0.2
Ce	0.4	0.8	0.5	NA	0.4	0.2	0.5	0.3	NA	0.3
	BCN-UB	POR-TR	FI-UB	MLN-UB	ATH-SUB	BCN-UB	POR-TR	FI-UB	MLN-UB	ATH-SUB
Secondary inorganic	4578	5072	3448	13147	5869	3316	3902	2724	9871	4004
Primary	7818	16966	7382	9851	6806	3574	10767	3748	7531	1884
POM+EC	2270	8257	4438	5918	853	2051	8586	3157	5795	663

Secondary	8619	9901	9734	25832	12081	6873	8746	9013	17876	9014
Sea salt	1494	4381	651	733	1655	380	1243	106	448	237
Mineral dust	4054	4341	2273	3790	4236	1144	2181	486	1286	986
Unexplained	6334	7792	1846	6188	1967	4762	6751	657	4449	966
Reconstructed	16192	26728	17050	31886	17815	10239	19929	12556	25680	10037

Table 2. Summary of input species, identified factors and constraints for city-specific PMF analyses.

Station	Input species	Sources/Factors	Constraints
BCN-UB	EC, OC, Al, Ca, Fe, K, Mg, Na, Cl^-, Ti, V, Cr, Mn, Ni, Cu, Zn, Li, Ga, As, Se, Rb, Sr, Cd, Sn, Sb, Ba, La, Ce, Pb, S, NH_4^+, NO_3^-	Vehicle exhaust (VEX), Vehicle non-exhaust (NEX), Secondary nitrate (SNI), Mineral (MIN), Secondary sulphate & organics (SSO), Industrial (IND), Heavy oil combustion (HOC) and Aged sea salt (SEA).	• Pulling the difference of source contributions between PM10 and PM2.5 to zero. • Pulling the chemical profile (24 species) of the NEX source towards the experimental profile of road dust obtained in Barcelona (Amato et al., 2009). • Pulling the ratios Cl^-/Na, S/Na, K/Na, Ca/Na, Mg/Na of the SEA profile to the literature values of 1.8, 0.084, 0.037, 0.038, 0.119 respectively.
FI-UB	EC, OC, Levoglucosan, Si, Al, Ca, Fe, K, Mg, Na, Cl, Ti, V, Cr, Mn, Ni, Cu, Zn, As, Se, Rb, Sr, Cd, Ba, Pb, S, Br, NH_4^+, NO_3^-	Aged sea salt (SEA), Saharan dust (SAH), Secondary sulphate & organics (SSO), Vehicle non-exhaust (NEX), Biomass burning (BB), Secondary nitrate (SNI), Vehicle exhaust (VEX), Heavy oil combustion (HOC), Local dust (LDU) and Fresh sea salt (FSS).	• Pulling down the EC and OC contributions in the SAH source profile and the NO_3^- contribution in the Sea Salt profile. • Pulling down the SAH source contributions during a period (1-22/07/13) when the advection of desert dust can be excluded on the basis of all the used transport models. • Pulling the difference of source contributions between PM10 and PM2.5 to zero, only for those days and sources where PM2.5 contribution was higher than PM10 contribution in the base run solution (55 days).
ATH-SUB	EC, OC, Si, Al, Ca, Fe, K, Mg, Na, Cl, Ti, V, Mn, Ni, Cu, Zn, As, Sr, Cd, Sb, Pb, S, Br, NH_4^+, NO_3^-	Heavy oil combustion (HOC), Vehicle exhaust (VEX), Secondary nitrate (SNI), Mineral (MIN), Vehicle non-exhaust (NEX), Biomass burning (BB), Secondary sulphate and organics (SSO) and Fresh sea salt (SEA).	• For the cases with daily PM2.5 contribution significantly higher than PM10 contribution, PM2.5 contribution was either set to zero (2 cases) or pulled down maximally (4 cases), depending on the respective PM10 contribution. • OC was pulled up in HOC factor • OC was set to have the original value of the unconstrained solution in the BB factor
POR-TR	EC, OC, Levoglucosan, Si, Al, Ca, Fe, K, Mg, Na, Cl^-, Ti, V, Cr, Mn, Ni, Cu, Zn, Li, As, Rb, Cd, Sn, Sb, La, Ce, Ba, Pb, S, Br, NH_4^+, NO_3^-	Biomass burning (BB), Secondary nitrate (SNI), Heavy oil and secondary sulphate (HOS), Mineral (MIN), Sea salt (SEA), Industrial (IND), Vehicle non-exhaust (NEX), and Vehicle exhaust (VEX).	• Pulling the difference of source contributions between PM10 and PM2.5 to zero, only for those days and sources where PM2.5 contribution was higher than PM10 contribution in the base run solution.
MLN-UB	EC, OC, Levoglucosan, Si, Al, Ca, Fe, K, Mg^{2+}, Na^+, Cl, Ti, V, Cr, Mn, Ni, Cu, Zn, Rb, Pb, S, Br, NH_4^+, NO_3^-	Vehicle exhaust (VEX), Vehicle non-exhaust (NEX), Mineral dust (MIN), Industrial (IND), Aged sea salt (SEA), Biomass burning (BB), Secondary nitrate (SNI) and Heavy oil combustion& secondary sulphate (HOS).	• Setting to zero the presence of levoglucosan in VEX and SEA factors. • Pulling down maximally the presence of Na^+ in the SNI factor. • In the SEA profile pulling the ratio Cl/ Na^+ to the literature value of 1.8.

Table 3. Average contribution (%) of PM10 and PM2.5 sources during high pollution days (PM10>50μg/m^3, and >40μg/m^3 in BCN-UB)

	BCN-UB		FI-UB		ATH-SUB		POR-TR		MLN-UB	
	PM10	**PM2.5**	**PM10**	**PM2.5**	**PM10**	**PM2.5**	**PM10**	**PM2.5**	**PM10**	**PM2.5**
Aged sea salt	2	1	<1	<1			3	<1	2	1
Saharan dust	<1	<1	<1	<1	52	45	<1	<1	<1	<1
Local dust	4	2	<1	<1	1	2	27	22	3	2
Sec. sulphate & organics	19	22	6	6	2	5	5*	2*	9*	11*
Vehicle non-exhaust	14	2	9	1	3	1	6	3	14	8
Vehicle exhaust	13	20	5	5	4	9	25	30	5	5
Heavy oil combustion	4	6	3	3	3	10				
Industrial	17	18			<1	<1	2	1	4	3
Secondary nitrate	27	29	36	32	3	4	7	3	28	34
Fresh sea salt			<1	<1	7	1				
Biomass burning			30	33	1	2	25	33	35	26
Unaccounted			8	20	24	21		5		10

*includes heavy oil combustion

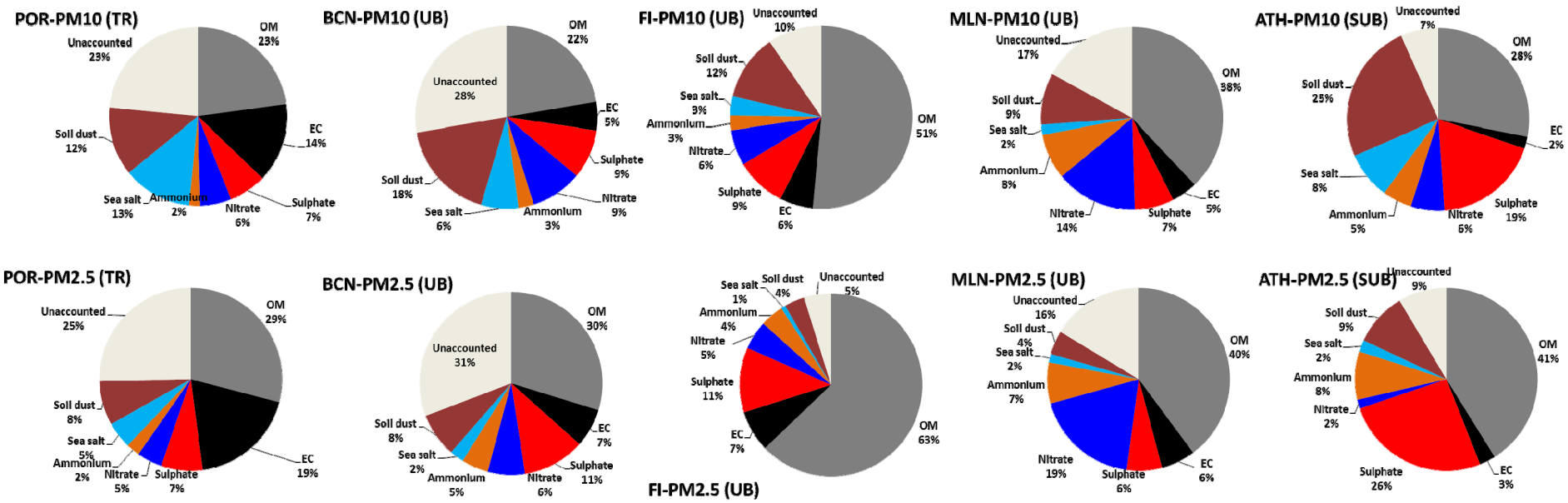

Figure 1. Mass closure of PM10 and PM2.5 chemical speciation data for the 5 AIRUSE cities.

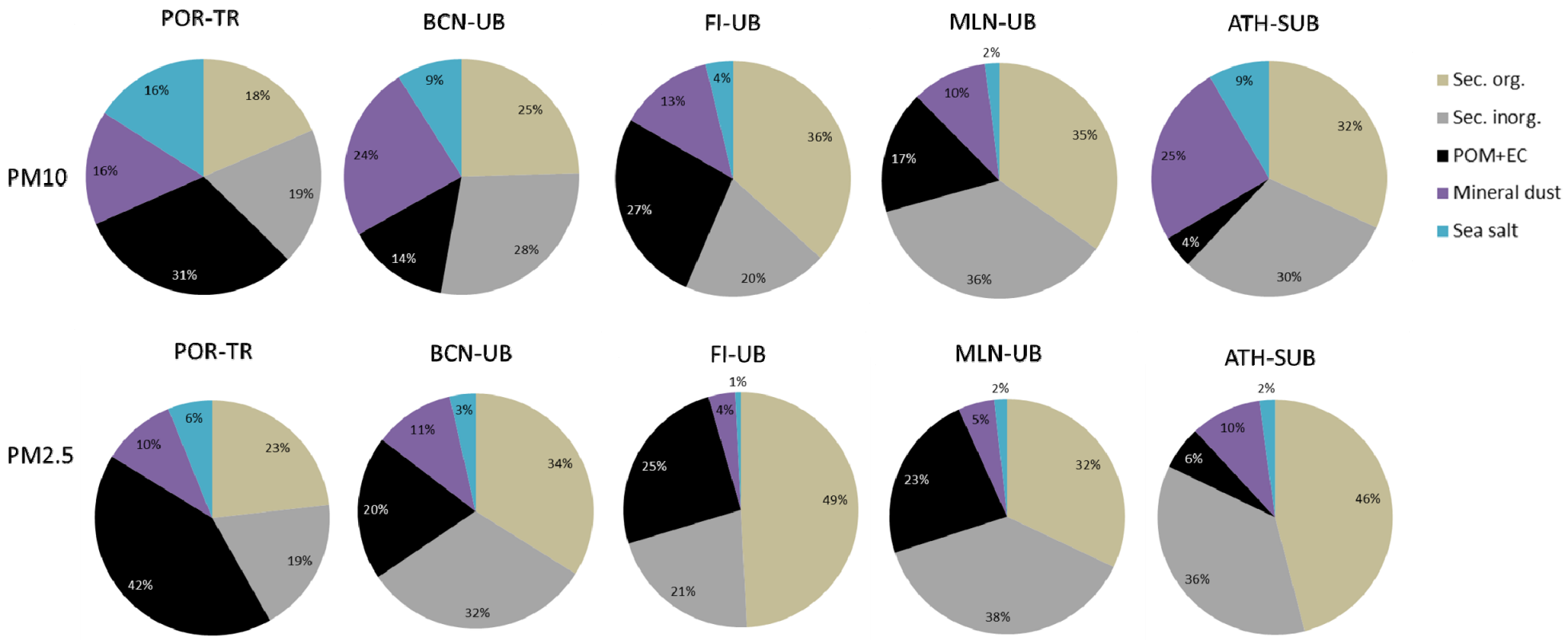

Figure 2. Secondary and primary PM components to the mean PM10 and PM2.5 levels at the 5 AIRUSE cities.

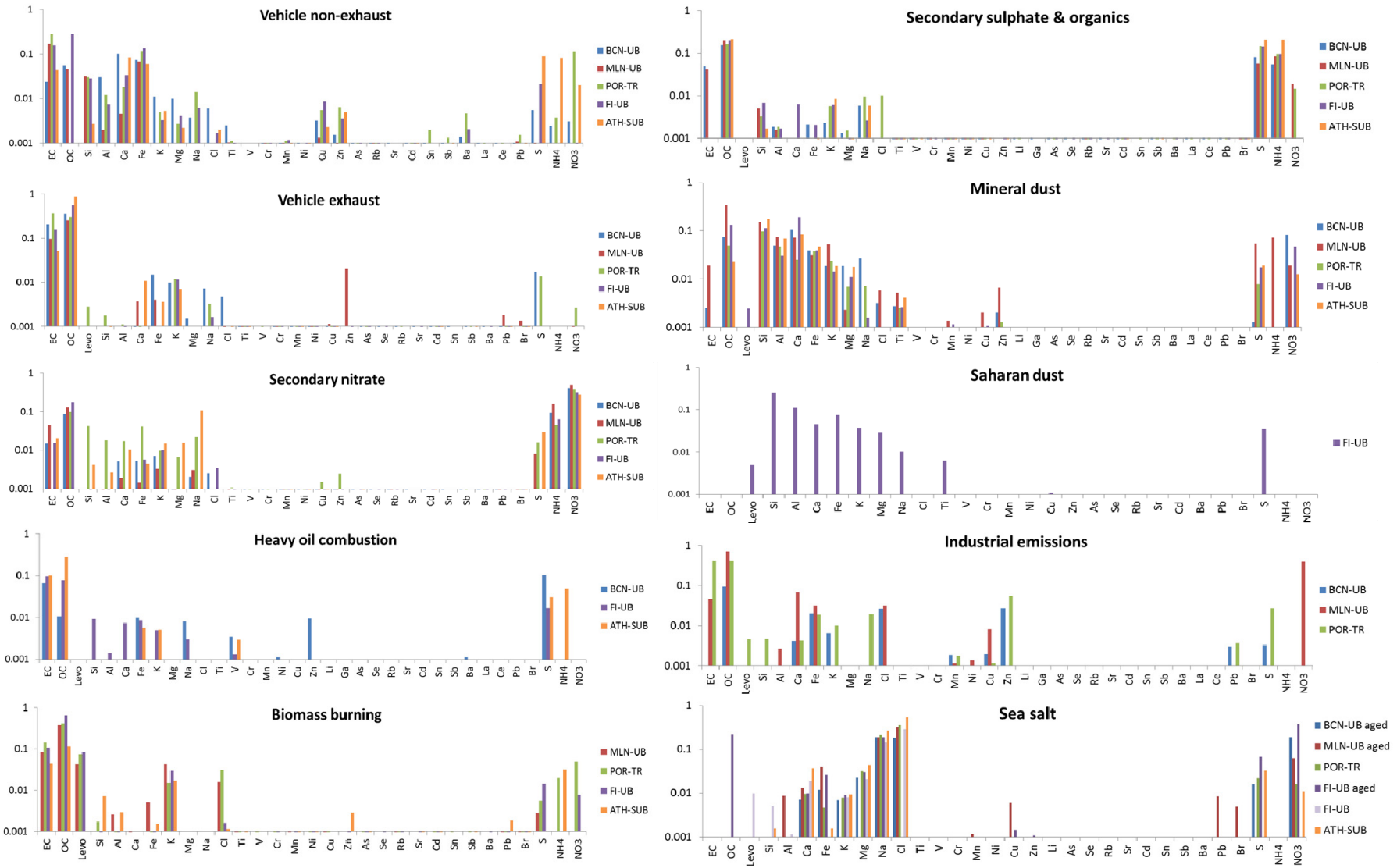

Figure 3. PMF factor profiles (μg/μg) for each monitoring site. At MLN-UB and POR-TR, the SSO factor includes heavy oil combustion.

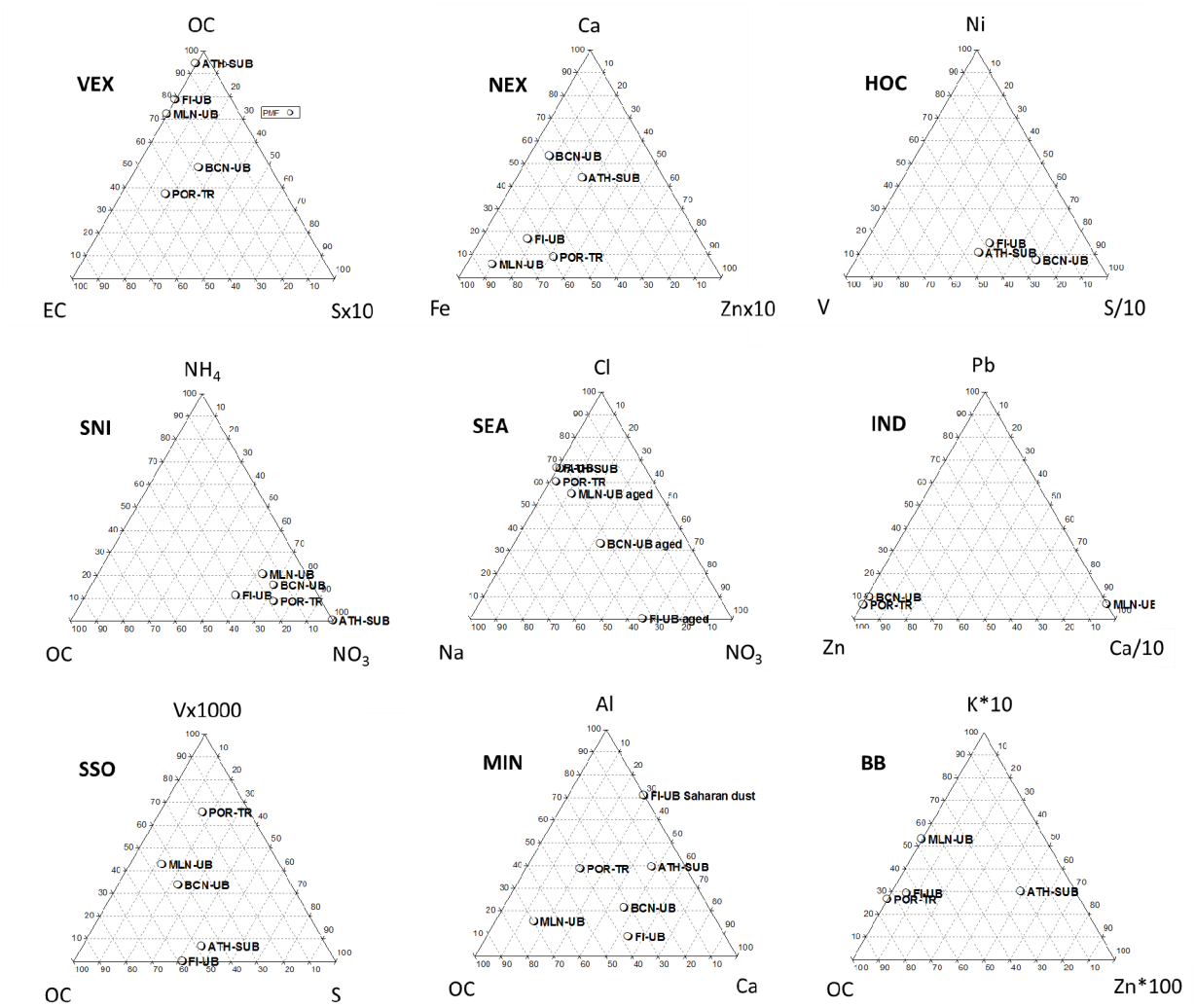

Figure 4: Ternary plots for PMF factor profiles.

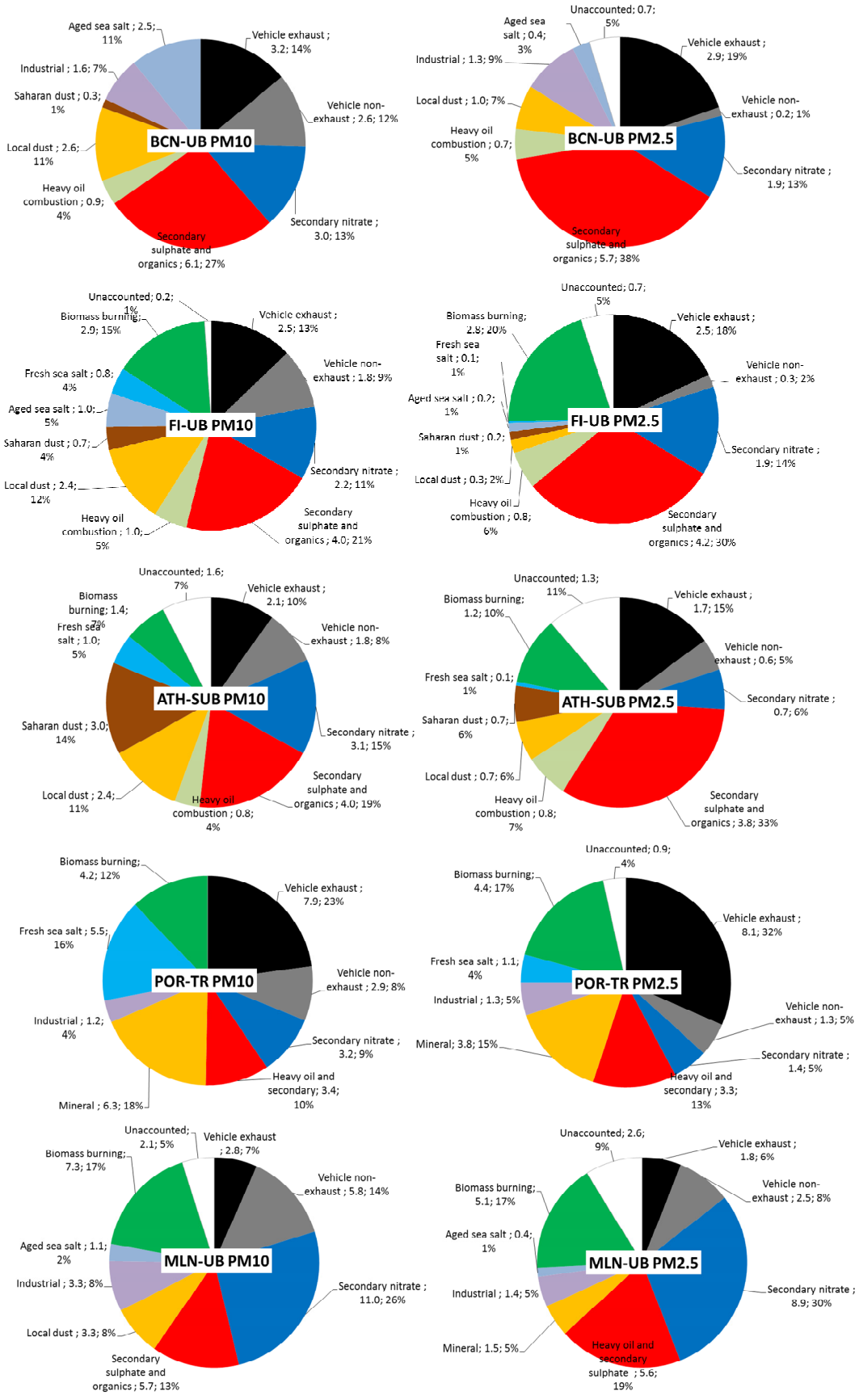

Figure 5. Average contribution (%) of PM10 and PM2.5 sources for 12 months study

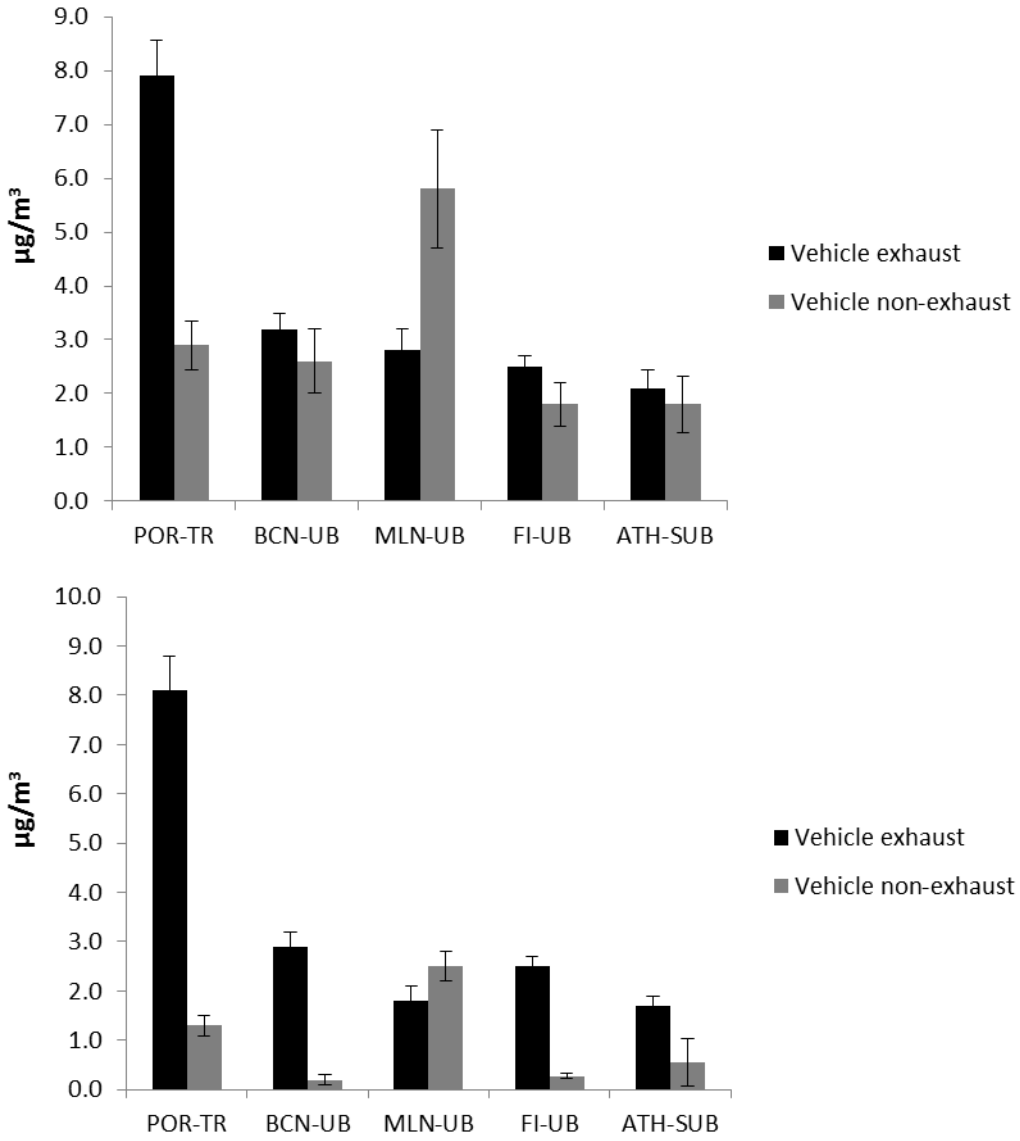

Figure 6. Mean contributions for traffic-related sources at the five AIRUSE cities for PM10 (top) and PM2.5 (bottom).Error bars are calculated based on the standard error of the coefficients of a multiple regression between the daily PM concentration and the source contributions. And do not include modelling errors.